NeuroImage 280 (2023) 120354

Contents lists available at ScienceDirect

NeuroImage

journal homepage: www.elsevier.com/locate/ynimg

Review

Quantification of inter-brain coupling: A review of current methods used in haemodynamic and electrophysiological hyperscanning studies

U Hakim [a,*], S De Felice [b,c], P Pinti [a,d], X Zhang [e], J . A Noah [e], Y Ono [f], P.W. Burgess [b], A Hamilton [b], J Hirsch [a,e,g,h], I Tachtsidis [a]

[a] Department of Medical Physics and Biomedical Engineering, University College London, Malet Place Engineering Building, Gower Street, London WC1E 6BT, United Kingdom
[b] Institute of Cognitive Neuroscience, University College London, London, United Kingdom
[c] Department of Psychology, University of Cambridge, United Kingdom
[d] Centre for Brain and Cognitive Development, Birkbeck, University of London, London, United Kingdom
[e] Department of Psychiatry, Yale School of Medicine, New Haven, CT, United States
[f] Department of Electronics and Bioinformatics, School of Science and Technology, Meiji University, Kawasaki, Kanagawa, Japan
[g] Departments of Neuroscience and Comparative Medicine, Yale School of Medicine, New Haven, CT, United States
[h] Yale University, Wu Tsai Institute, New Haven, CT, United States

ARTICLE INFO

Keywords:
Hyperscanning
Social neuroscience
Interbrain interaction
Two person neuroscience
Dyadic neuroscience
Neuroimaging
Interbrain synchrony

ABSTRACT

Hyperscanning is a form of neuroimaging experiment where the brains of two or more participants are imaged simultaneously whilst they interact. Within the domain of social neuroscience, hyperscanning is increasingly used to measure inter-brain coupling (IBC) and explore how brain responses change in tandem during social interaction. In addition to cognitive research, some have suggested that quantification of the interplay between interacting participants can be used as a biomarker for a variety of cognitive mechanisms aswell as to investigate mental health and developmental conditions including schizophrenia, social anxiety and autism. However, many different methods have been used to quantify brain coupling and this can lead to questions about comparability across studies and reduce research reproducibility. Here, we review methods for quantifying IBC, and suggest some ways moving forward. Following the PRISMA guidelines, we reviewed 215 hyperscanning studies, across four different brain imaging modalities: functional near-infrared spectroscopy (fNIRS), functional magnetic resonance (fMRI), electroencephalography (EEG) and magnetoencephalography (MEG). Overall, the review identified a total of 27 different methods used to compute IBC. The most common hyperscanning modality is fNIRS, used by 119 studies, 89 of which adopted wavelet coherence. Based on the results of this literature survey, we first report summary statistics of the hyperscanning field, followed by a brief overview of each signal that is obtained from each neuroimaging modality used in hyperscanning. We then discuss the rationale, assumptions and suitability of each method to different modalities which can be used to investigate IBC. Finally, we discuss issues surrounding the interpretation of each method.

1. Introduction

Social interactions are a fundamental aspect of human existence, from the interactions between a child and their parent, to world leaders on the global stage. The nature and quality of social interaction is strongly related to mental well-being (Schilbach, 2016). Quantifying and, therefore, improving our understanding of social interactions is therefore an important goal of neuroimaging in social neuroscience.

Traditional neuroimaging studies in cognitive neuroscience use 'single-brain' experiments where a participant is given a task to complete while their neural activity is recorded. However, whether this form of experiment is able to provide a meaningful picture of real world social interactions is unclear. We know that people behave differently when in a social interaction, (Becchio et al., 2010) and when being watched (Hamilton et al., 2016), and the interactions of a participant with a trained confederate may not capture natural behaviour (Kuhlen and Brennan, 2013). Thus research into real world social behaviour may require researchers to place two or more naïve participants in an

* Corresponding author.
E-mail address: uzair.hakim.17@ucl.ac.uk (U. Hakim).

https://doi.org/10.1016/j.neuroimage.2023.120354
Received 8 July 2023; Received in revised form 25 August 2023; Accepted 28 August 2023
Available online 4 September 2023
1053-8119/© 2023 The Authors. Published by Elsevier Inc. This is an open access article under the CC BY license (http://creativecommons.org/licenses/by/4.0/).

interaction. In this context, capturing data from all participants with hyperscanning may allow new and distinctive types of analysis, compared to the study of one brain at a time. Hyperscanning allows researchers to capture the association between multiple individual participants' neural data as they take part in a paradigm together.

In this review, we include within the definition of hyperscanning any form of 'interaction', where this is some degree of reciprocity, between scanned participants, including computer-based interaction (e.g. (Montague et al., 2002; King-Casas et al., 2005; Bilek et al., 2015)) as well as face-to-face interaction (e.g. (Dravida et al., 2020; Noah et al., 2020; Cañigueral et al., 2021; Hirsch et al., 2021, 2022)). The core feature of hyperscanning is that data is collected simultaneously from more than one participant and those participants have some means of exchanging information between them. This directly contrast to sequential acquisition of data from participants who experience the same events (watching a movie for example) but are scanned separately and analysed together (e.g. (Hasson et al., 2004)). This contrast is displayed visually in Fig. 1. In the sequential case, researchers can measure 'intersubject correlations' or 'neural alignment', which indexes if different brains respond in the same way to a given experience (Sievers et al., 2020), but this cannot provide any information about dynamic interactions between data acquired from interacting participant brains.

Beyond simple 'neural alignment' (inter-brain similarity to a given experience) available from sequential neuroimaging, hyperscanning paradigms measure complex dynamics between interactive brains, as they continuously and mutually adapt over their interaction. The cognitive interpretation of the IBC signal is still debated, with models focusing on coupling (Hasson and Frith, 2016), responses to the shared environment (Holroyd, 2022) and mutual prediction (Hamilton, 2021). Some studies give richer interpretations, suggesting that IBC might provide a biomarker for social connectedness (Hoehl et al., 2021) or attunement (Gvirts and Perlmutter, 2020) but it is not yet clear if these can be supported. Importantly, as interactions are complex, signals from multiple interactive brains may not necessarily 'mirror' each other, but would instead 'couple' to each other dynamically over time (Hasson & Frith, 2016). Understanding this dynamic calls for more complex analysis tools that are able to capture relevant components from this type of data.

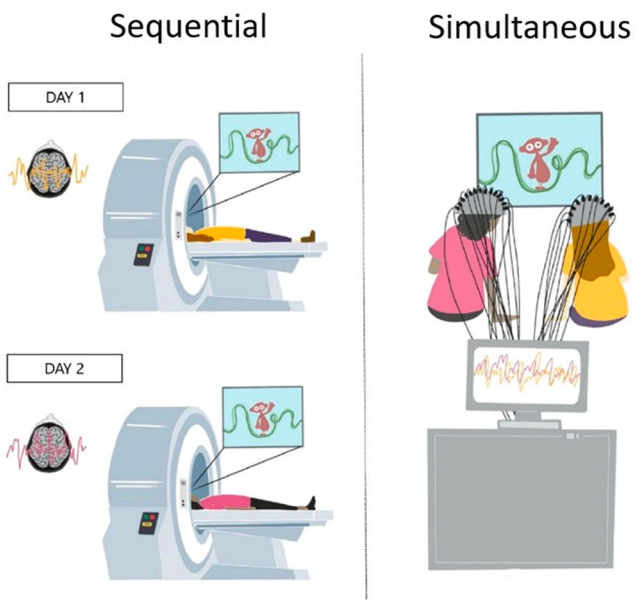

Fig. 1. Left: Participants watch the same clip while receiving an fMRI scan on different days. The neural responses from both participants are compared. The output can only give information about similarity of neural responses to a given experience. Right: Participants watch the same clip, at the same time, whilst neural responses are recorded simultaneously. The output can provide information about the real-time interaction between participants.

In a field that is rapidly expanding, a wide variety of methods have been used to compute the IBC, with inconsistency across studies. Understanding what each analytic method can (and cannot) explain about the data from hyperscanning studies is important to achieve a coherent and robust advancement of the field. This is particularly relevant when claims are made that IBC may reflect specific cognitive mechanisms (e.g. (Osaka et al., 2015; Goelman et al., 2019; Dravida et al., 2020; Ono et al., 2021)), developmental disorders (Hasegawa et al., 2016; Wang et al., 2020; Kruppa et al., 2021; Key et al., 2022) or could provide a metric for psychiatric treatment (Leong and Schilbach, 2019). This review aims to clarify some of this confusion and provide some clarity about the several methods used to analyse and interpret hyperscanning data within the social neuroscience domain.

To date there have been 19 review papers focusing on various aspects of hyperscanning (Dumas et al., 2011; Konvalinka and Roepstorff, 2012; Scholkmann et al., 2013; Babiloni and Astolfi, 2014; Koike, Tanabe and Sadato, 2015; Acquadro, Congedo and De Riddeer, 2016; Crivelli and Balconi, 2017; Liu et al., 2018; Wang et al., 2018; Quaresima and Ferrari, 2019; Balters et al., 2020; Czeszumski et al., 2020, 2022; Nam et al., 2020; Misaki et al., 2021; Müller, Ohström and Lindenberger, 2021; Shemyakina and Nagornova, 2021; Kelsen et al., 2022; Tsoi et al., 2022). Previous reviews have focused on hyperscanning in the context of specific modalities, including functional near-infrared spectroscopy (fNIRS) (Scholkmann et al., 2013; Quaresima and Ferrari, 2019; Balters et al., 2020; Czeszumski et al., 2022), electroencephelaography (EEG) (Liu et al., 2018) or functional magnetic resonance imaging (fMRI) (Misaki et al., 2021; Tsoi et al., 2022). In terms of cognitive neuroscience issues, previous reviews have generally focused on social cognition as a whole, compiling studies investigating imitation and joint action, coordination and competition, emotion, speech and communication and a variety of other components of social cognition. However, some reviews have focused on specific components of cognitive neuroscience such as imitation and joint action (Dumas et al., 2011), joint action, shared attention, interactive decision making and affective communication (Liu et al., 2018), imitation, coordination, eye contact, game theory, cooperation and competition (Wang et al., 2018), education, decision making, motor synchronization (Nam et al., 2020) cooperation and competition (Shemyakina and Nagornova, 2021) or spoken communication (Kelsen et al., 2022).

Taken together, all the reviews mentioned above tend to focus on the interpretation of IBC (results/outputs), while largely neglecting how the IBC measure is computed (methods). There are however two which have both dedicated some sections to analytic methods and principles (Czeszumski et al., 2020; Tsoi et al., 2022). But one is limited in that it only includes fMRI hyperscanning studies (Tsoi et al., 2022), while the other (Czeszumski et al., 2020) covers only some of the methods that have been used, and discusses them within macro-categories rather than in detail (e.g. 'coupling/connectivity measures', 'correlation and dependendance analyses' etc). So the present review extends previous work by (i) systematically reviewing all methods used to compute IBC in all hyperscanning studies (including several different neuroimaging modalities), and (ii) expanding each macro-category and discussing each method separately (e.g. Pearson correlation is discussed separately to cross-correlation). Specifically, the present review considers the implications of each method applied to hyperscanning data, with a focus on its technical aspects, including the rationale, mathematical assumptions and its suitability for a given modality. The aim of this review overall is to provide a comprehensive outline of the methods currently used across neuroimaging modalities and consider the rationale and mathematical assumptions of each method behind the computation of IBC.

The structure of the review is as follows. First, we discuss the method we used to search the literature, along with the removal criteria to preserve the replicability of the review for future updates. We then provide a current summary of the state of the field, including number of papers published, methods and modalities used. Following this, we

provide a brief summary of the signal characteristics of different neuroimaging modalities. The metrics of IBC are then reviewed where we cover the rationale of each method, in its original form and its application to hyperscanning, the mathematical assumptions when using each method, what the method can explain about the relationship between input data, the suitability of the method to different modalities and finally which modalities it has been applied to. The discussion will summarize our review of the methods with a brief discussion on the importance of clarity of method used, issues surrounding interpretability and frequency selection. Finally we conclude with our perspective on the future of computational methods within hyperscanning studies, to improve hyperscanning investigations and derived metrics, and ultimately achieving a better understanding of how IBC can be used to shed light on the mechanisms supporting social interactions.

2. Methods

This work was carried out according to the Preferred Reporting Items for Systematic Reviews and Meta-Analyses (PRISMA) guidelines (Liberati et al., 2009), to increase the replicability of this review. Studies utilizing hyperscanning were discovered through searches on PubMed and Scopus, using the search terms: (hyperscanning[Title/Abstract] OR two person neuroscience[Title/Abstract]) AND (fmri[Title/Abstract] OR eeg[Title/Abstract] OR fNIRS[Title/Abstract] OR MEG[Title/Abstract] OR nirs[Title/Abstract])) and (hyperscanning OR "two person neuroscience") AND (fnirs OR nirs OR eeg OR fmri OR meg), for PubMed and Scopus respectively. The years of interest range from 2000 (two years prior to the seminal hyperscanning paper by Montague et al. (2002)) to the end of 2022. Initial search was carried out for journal articles published in the English language, searching paper titles and abstracts only. Following the PRISMA recommendation to follow the PICOS (Population, Intervention, Comparator, Outcomes, Study designs) eligibility criteria, these were defined before conducting the title and abstract screening and are listed in Table 1.

Populations (for example, neurodivergent populations) were not restricted since the focus of this review is on the quantification of the IBC parameter and not on clinical conditions. Hyperscanning requires participants to be scanned simultaneously to allow transient interacting dynamics to be probed and therefore any studies where the participant data was acquired and analysed sequentially were excluded. Interventions in this context refer to imaging modality, hyperscanning is possible with all functional neuroimaging modalities, therefore no restrictions were placed on this criteria. Comparators require that two brains are scanned, it was not important whether the study compared neurodivergent to neurotypical, or any other comparison. Outcomes of studies must include a quantification of IBC. Finally, any study design was included aslong as data were acquired simultaneously.

Initial search provided a total of 659 documents, after duplications were removed, 354 documents were examined further. Only published, original, research articles were considered for review, and a further 116 documents were removed due to being review papers, meta-analyses, conference papers, book chapters, erratum, meeting abstracts, notes, surveys, not in English or the full text being unavailable. The PICOS eligibility criteria from Table 1 was first applied to the title and abstracts and a further 37 papers were removed (P: 11, C:4, O:22). During text screening a further 5 were removed (P:1, O: 4). Review papers were mined for papers missed in the initial database search and 19 papers were added from this. The final count of papers considered was 215. The PRISMA flowchart is shown in Fig. 2.

Table 1
PICOS eligibility criteria used to filter papers found from initial search.

Criteria	Requirements
Population	Participants interacting and scanned simultaneously
Intervention	fNIRS, EEG, fMRI, MEG or any combination
Comparators	Scanning two or more brains
Outcomes	Inter-brain dynamic analysis
Study Design	Standard cognitive neuroscience protocols

Methods were broadly grouped according to the categories provided by Ayrolles et al. (2021) for their Python based Hyperscanning toolbox, with the addition of the 'Regression' category. In total five categories were identified. These are listed and defined in Table 2:

It should be noted that membership of a method to a specific category does not mean it only exists within that category (for example, Partial Directed Coherence can be in both Causal and Coherence based methods); categorisation is only a way to group for ease of discussion.

3. Summary statistics

The number of hyperscanning papers published since the seminal work by Montague et al. (2002) has steadily increased year-on-year since 2014, reaching a peak of 46 publications in 2022 (Fig. 3(a)). This consistent increase is likely tied to the increase in computational power to process data more efficiently, and more importantly the availability of more affordable neuroimaging equipment. Four neuroimaging techniques have been used for hyperscanning: fNIRS, fMRI, EEG and MEG. The breakdown of publications by modality per year is shown in Fig. 3(b).

In fact, from Fig. 3(b), it is clear that more affordable neuroimaging methods such as EEG and fNIRS have become the modality of choice, with fNIRS being the modality used for the majority of papers since 2015.

Fig. 4 shows the number of published papers for each analytic category, by neuroimaging technique. The properties of data acquired from different neuroimaging techniques makes some methods more applicable to certain data compared to others. For example, the high temporal resolution of EEG data makes it more suitable for Phase Synchrony analyses than fMRI.

In terms of populations, 83% of studies reviewed conducted hyperscanning with adult (18 years or older) populations, and a further 8% conducted adult-infant studies where a parent interacted with their child, 4% conducted either infant-infant interactions, or adult-adolescent and 5% did not state the age demographics. In addition 72% of the hyperscanning experiments investigated neurotypical populations (26% did not state if participants had any medical conditions).

4. Signal characteristics of neuroimaging modalities

Each functional neuroimaging technique can be classified as either a direct or indirect measure of brain activation. EEG and MEG measure the direct electrical and magnetic outputs arising from synaptic activity during a period of active brain function. In comparison fNIRS and fMRI are indirect measures monitoring a change in oxygenation of blood flow to infer brain activation, fNIRS monitors the optical properties, whilst fMRI detects the change in magnetic properties. Given the difference in biological and physical properties recorded, the signals acquired from each modality vary interms of their characteristics. This has an effect on what analytic method can be effectively used to determine IBC. In this section we briefly discuss the properties of the signal acquired from each modality (Table 3).

4.1. Functional near-infrared spectroscopy (fNIRS)

fNIRS data is recorded using pairs of optodes which comprise a recording channel. One of these optodes is a source emitting near-infrared (NIR) light, whilst the other is a detector which detects the emitted NIR light after it has travelled through the cortex. The source and detectors are typically spaced 3 cm apart to ensure the light is able to penetrate to the cortex, without becoming too diffuse. As a result of this the spatial resolution is inherently limited to the cm scale, additionally the light can only reach the cortical surface (~1.5 cm from the

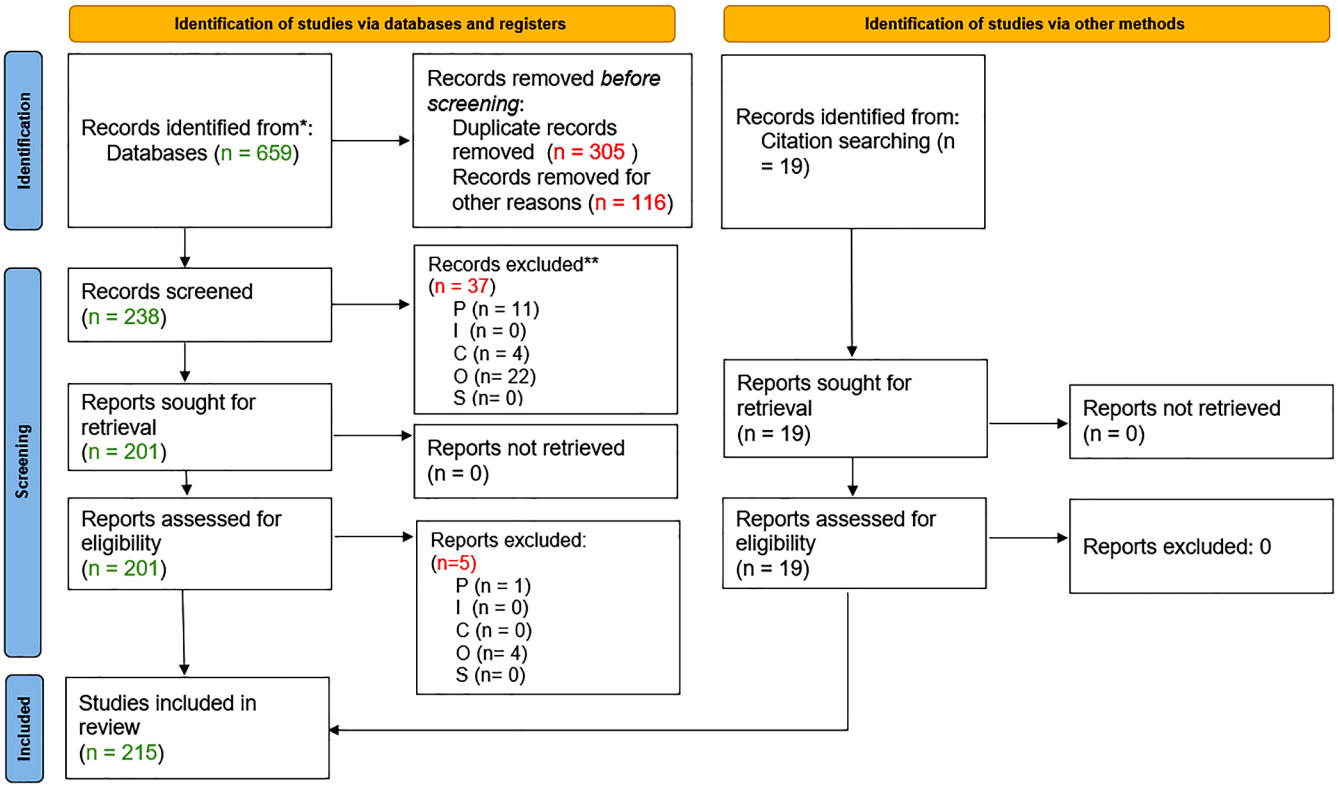

Fig. 2. PRISMA flowchart for paper exclusions. Flowchart adapted from (Page et al., 2021). Numbers highlighted in red are how many papers are removed, whilst green are included at each stage.

Table 2
Categories of methods used to compute IBC and their meaning.

Category	Measurement
Correlation	Temporal similarity between participant data.
Regression	Linear regression to relate participant data to one another.
Coherence	Frequency/Time-frequency similarity between participant data.
Phase Synchrony	Assess phase relationship between data.
Causality	Causal inference from one participant data to another.

scalp) (Pinti et al., 2020) and so fNIRS is unable to image deep brain structures. The indirect mechanism of measurement for fNIRS means the recorded functional activation is essentially a proxy of biological functional activation. The mechanism which is recorded is the haemodynamic response function (HRF). The HRF manifests over a period of seconds, and is slower than the direct, postsynaptic response which typically occurs on a millisecond scale. Hence, very fast changes in the brain are undetectable using fNIRS. This speaks to the temporal resolution of fNIRS systems, which is usually around 10Hz which oversamples the slow occurring HRF providing adequate temporal resolution for the biological phenomena it is imaging. Since fNIRS is an optical technique, the light must pass through non-neuronal tissue before arriving at the cortex of the brain. As a result the changes detected by the system may be arising from neuronal changes elicited from the stimulus aswell as non-neuronal changes related to participant physiology. This is a well known and discussed issue in fNIRS and the inclusion of physiological monitoring is recommended to allow for a indepth division of evoked neuronal changes from non-evoked systemic changes (Obrig and Villringer, 2003; Kirilina et al., 2012; Scholkmann et al., 2014; Tachtsidis and Scholkmann, 2016; Guglielmini et al., 2022). The frequency components present in the fNIRS signal have been well characterized, typically the evoked neuronal component occurs at approximately 0.025 Hz (although is dependent on the rate of stimulus presentation), whilst Mayer waves occur at approximately ~0.09 Hz, breathing rate at ~0.25 Hz and heart rate at ~1.3 Hz (Pinti et al., 2019). Therefore when analysing fNIRS data special attention should be paid to the frequency of interest and care should be taken to ensure the task-stimulus frequency does not overlap with physiological components. This can easily be done by ensuring any repeated task blocks do not occur at a rate overlapping with any of the frequencies mentioned above. In addition to systemic noise, fNIRS is also susceptible to signal contamination from ambient light in the recording room and interference from participant hair, both of which can be avoided with careful participant setup.

4.2. *Electroencephalography (EEG)*

EEG uses an array of electrodes to detect small electrical potentials at the scalp which are linked to the firing of neurons in the brain. While the spacing of EEG electrodes is typically 2 and 3 cm apart, spatial resolution is much lower. This is because the human head conducts electricity (a phenomena known as volume conduction) and therefore localizing signals to a specific origin is difficult, or impossible. Spatial localisation therefore may be 5–15 cm and depth cannot be easily determined. A larger challenge for researchers is movement artefacts, as any movement of the eyes, face or jaw of a participant will cause large and variable artefacts in the EEG signal which are not easy to remove. This is particularly challenging in hyperscanning studies of natural social interaction where the task allows participants to move and speak freely (Marriott Haresign et al., 2021). In contrast to low spatial resolution the direct nature of the originating signal means the temporal resolution of the EEG signal is extremely fine grained, and transient changes in neuronal signals occurring from small changes in behaviour are detectable using EEG. Typically EEG systems have sample rates of 1 kHz upwards to adequately sample the faster frequencies of the brain data. Since EEG records direct electrical signals the signal is not contaminated by other physiological noise, and the frequency components of the EEG signal all directly relate to brain function. These frequencies have been well characterized and grouped into bands: Delta (1–3 Hz), Theta (4–7

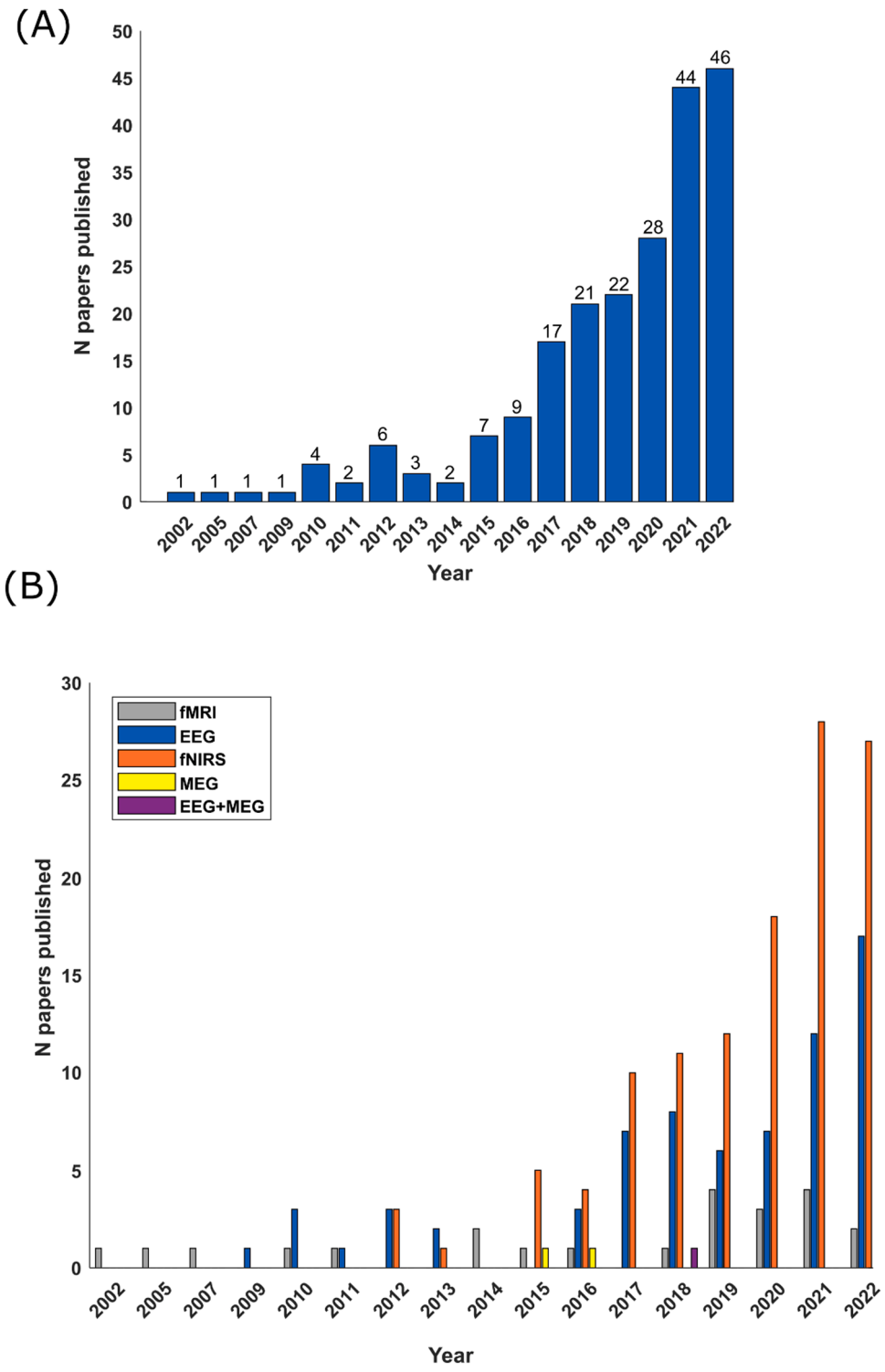

Fig. 3. (a) Number of hyperscanning studies published in total per year. (b) Number of hyperscanning studies published per year per neuroimaging technique.

Hz), Alpha (8–12 Hz), Beta (13–30 Hz), Gamma (30–100 Hz) (Saby and Marshall, 2012).

4.3. Functional magnetic resonance (fMRI)

The fMRI blood oxygenation level dependent (BOLD) signal is an indirect measure of neuronal activity, which detects the change in paramagnetism of haemoglobin depending on its oxygenation state. fMRI is widely used in cognitive neuroscience and has excellent spatial resolution, with typical scanners providing approx. 3mm voxels throughout the brain with precise localisation of activation to anatomical structures. The HRF used to determine functional activation is the same biological phenomena that is imaged by fNIRS and so suffers the same delay. However, the temporal resolution of fMRI systems is slower than fNIRS, since the typical MRI sequence used to obtain fMRI data (Echo Planar Imaging) acquires a sample every 2 seconds. In this respect the temporal resolution is worse than fNIRS even though the physiological basis for functional activation is the same.

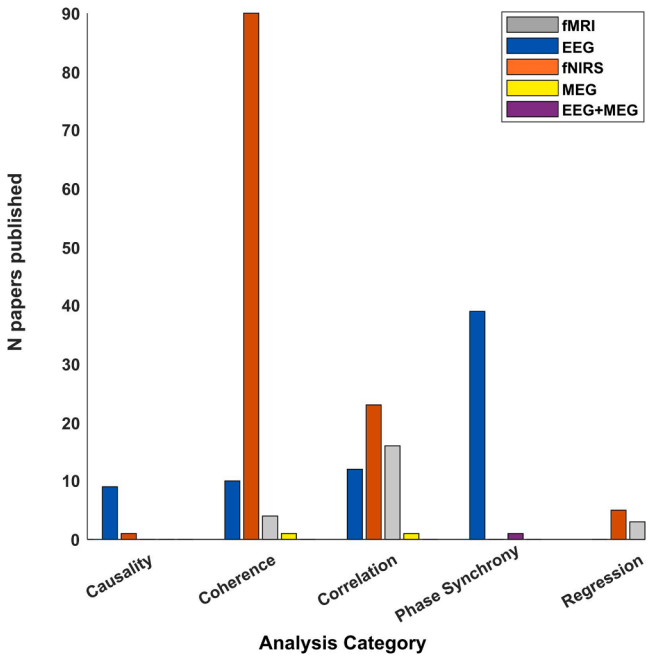

Fig. 4. Number of papers published for each analysis category for each neuroimaging technique.

Table 3
Recording properties of each neuroimaging technique used in hyperscanning experiments. Biological property refers to the underlying physiological phenomena the modality images, whereas physical property refers to what parameter of the biological property the modality exploits to obtain the data.

Modality	Direct/Indirect	Biological Property	Physical Property
fNIRS	Indirect	Haemodynamic Response	Optical
EEG	Direct	Postsynaptic Potential	Electrical
fMRI	Indirect	Haemodynamic Reponse	Magnetic
MEG	Direct	Postsynaptic Potential	Magnetic

Like fNIRS, the fMRI signal can be contaminated by physiological noise, however the origin of the noise is mainly due to motion induced from physiology, such as pulsatility of blood flow which induces noise around large arteries and draining veins, whilst thoracic movements from breathing also induce changes in the head which produce a shift in the phase of the image (Caballero-Gaudes and Reynolds, 2017). A further limitation, which is particularly important for hyperscanning research, is that MRI is sensitive to participant movement and requires participants to lie down and remain still in an enclosed and noisy environment. Hyperscanning requires two participants in separate room to be linked via computer interfaces, and are not conducive to a natural social interaction. In particular the lack of spontaneous movement from participants means the fMRI imaging environment is highly 'artificial' (not ecologically valid) and investigating social interactions with loud scanner noise in the background, whilst laying down is perhaps unrepresentative of the interactions hyperscanning seeks to investigate.

4.4. Magnetoencephalography (MEG)

The origination of MEG signals are the same as EEG; the postsynaptic electrical current is accompanied by a magnetic field, in which fluctuations are detected by the MEG sensors. As a result of it recording the direct synaptic response the temporal resolution of MEG data is comparable to EEG, and the frequency components composing the signal are in line with EEG; Theta: 4–8 Hz, Alpha: 9–14 Hz, Beta: 15–30 Hz, Gamma: 30 Hz+ (Niedermeyer and Silva, 2005) and the typical sampling rate for an MEG system is similarly as high as EEG. The spatial localization of MEG data requires solving an inverse problem to determine the source space of the data, this is considered the main challenge of MEG data and therefore has an implication on the spatial resolution of the acquired MEG data. The low magnetic permeability of tissue allows the magnetic field originating from the brain to travel through the skull and scalp with no interference, meaning MEG data is not susceptible to effects of volume conduction. Magnetic interference from equipment in the room can cause interference in the data but is typically easily filtered using low pass frequency domain filters. However, face and eye movements can still cause artefacts. While participants in MEG are typically seated with a larger field of view than MRI, their movements are still constrained and typical hyperscanning studies rely on computer interfaces (Zhdanov et al., 2015). Newer OP-MEG systems (Holmes et al., 2023) potentially allow for MEG hyperscanning in interacting participants, but studies are still constrained to a shielded room with minimal movements.

4.5. Frequency Components used in hyperscanning studies

As discussed above, different modalities record different physiological phenomena, and therefore, frequency components within each signal reflect different things. Broadly these can be divided between the electromagnetic modalities; EEG and MEG, and the haemodynamic modalities; fMRI and fNIRS.

Within EEG and MEG the frequency components divided into bands (Delta, Theta, Alpha, Beta, Gamma) reflect varying processes in the brain depending on context and location. In this review the studies using EEG (71 total) analysed varying frequency bands, these are summarised in Table 4.

39 studies analysed multiple frequency bands. The 22 'other range' did not specify any frequency bands as defined in the EEG literature, but did specify some range of frequencies. One of the two MEG studies analysed Delta wave frequencies, whilst the other analysed Alpha band for both adults and infants.

When analysing frequency bands for haemodynamic signals, the main requirement is to exclude frequencies associated with non-neuronal physiological responses. Typically experimenters analyse frequencies close to the task-frequency; the frequency at which task stimulus is presented. Of the 23 fMRI studies included in this review, 5 studies analysed a range of frequencies (0.0025–0.02, 0.008-0.009, 0.008–0.45, 0.01–0.8,0.645–1), whilst 17 analysed a single specific frequency component, given in Table 5.

Of the 119 fNIRS studies included in this review, 12 did not specify any information about the frequencies that were examined. All 107 remaining studies focused on a range of frequencies for their analysis. The mean of the minimum frequencies analysed was 0.067 Hz (standard deviation 0.135 Hz), whilst the mean of the maximum frequencies analysed was 0.3808 Hz (s.d. 0.6903 Hz).

5. Systematic review of metrics of IBC

Below we discuss the metrics used to investigate the relationship between participant neural data in hyperscanning studies, organised by categories. For a full list of studies and which methods they used, please refer Table 6 below. Where relevant, formulae are provided in the supplementary materials. In this section the input data for each method is the neural data from participants taking part in a simultaneously-

Table 4
Number of papers using each EEG frequency band. Papers which used multiple frequency bands are accounted for in each frequency band they have used.

Frequency band (Hz)	Delta (1-3)	Theta (4-7)	Alpha (8-12)	Beta (13-30)	Gamma (30+)	Other range
N studies	13	39	43	37	23	22

Table 5
Frequency components used for fMRI hyperscanning studies.

Frequency (Hz)	0.04	0.0625	0.29	0.33	0.4	0.435	0.5	0.645	1	1.4
N studies	1	1	1	1	1	2	7	1	1	1

imaged-hyperscanning paradigm. For studies using fMRI this is the BOLD signal, whilst EEG is the evoked potential and MEG is the magnetic field fluctuations. Since fNIRS provides both HbO_2 and HHb, studies can use either, both, or a combination of the two. The pros and cons of which signal to use is outside the scope of this paper and so data acquired using fNIRS will be referred to as fNIRS data, with no specification as to which signal. For further information with regards to signal performance and the benefits of using different signals please refer to (Kirilina et al., 2012; Tachtsidis and Scholkmann, 2016; Hakim et al., 2022).

For each method we will first state the property of input data that the method uses to determine IBC and the domain (time, frequency or time-frequency) it is applied to. Following this, we will outline the rationale behind each method as applied to hyperscanning, and as described by the original authors of the method where possible, along with the mathematical assumptions behind the use. Next we will consider mathematical considerations, including linearity, symmetry and its bi/multivariate nature. Finally the suitability of the method applied to each modality will be considered based on the temporal and spatial resolution of the measured signal, followed by which modalities have used the method.

Fig. 5 shows a representation of how hyperscanning metrics from each category are represented visually. The figures are examples of how hyperscanning data can be represented. Fig. 5 (a) shows how (Cheng et al., 2022) represents Pearson correlation of fNIRS data between participants. The representation to the left shows the t-value maps of correlation values, whilst the right shows the variation in Pearson product moment correlation values for their experimental groups as the task progresses. Figure 5 (b) is the representation of cross brain GLM from (Pinti et al., 2021). The magenta boxes show the t-values of a specific fNIRS channel at varying time-lags, whilst the blue boxes show the beta values. Fig. 5 (c) is the representation of wavelet coherence from (Wu et al., 2021) displaying the wavelet coherence spectrogram of a specific fNIRS channel from their two experimental groups (only-child and children with siblings). The increased coherence values in the non-only-child group is highlighted for a specific frequency band in red. Fig. 5 (d) shows the interbrain phase coherence from study by (Müller and Lindenberger, 2022) displaying the time-frequency diagrams on the left and the topological distributions of strength of interbrain phase coherence. Fig. 5(e) shows the representation of causal connections using multi-variate Granger causality from (Sciaraffa et al., 2021). The connections in green represent the between-subjects connectivity, with the thickness of the connection representing the percentage of couples which have the significant connection. The distribution plot on the left displays the density of between subject connections.

5.1. Correlation

Arugably the most fundamental form of investigating an interaction between neural data is to determine the correlation between them. 7 different forms of correlation were found: Pearson Correlation, Cross-Correlation, Partial Correlation, Spearman Rank Correlation, Beta Series Correlation, Dynamic Time Warping and Amplitude Envelope Correlation. 4 studies (Krueger et al., 2007; Saito et al., 2010; Holper et al., 2013; Shaw et al., 2018) did not state the type nor provided formulae for which correlation was used.

5.1.1. Pearson correlation

The Pearson Correlation Coefficient (PCC) (Eq.S1) examines how two variables (typically neural data originating from homologous regions on participants) co-vary together, typically in the time domain. The rationale of the correlation is that variables which are related should co-vary together, and so computing the PCC of the two variables quantifies the extent to which changes in one variable influence the other variable. The application of this rationale to hyperscanning studies is clear – if participants are 'interacting' their neural signals should vary together in some form. Typically this manifests as an increase in PCC from rest/non-interaction to task/interaction, and means the task is eliciting a neural interaction. There is an assumption of a linear relationship between input data, therefore if the relationship is highly non-linear the PCC will be low. Secondly, the data are normally distributed, however the PCC is generally robust to non-normal distributions as long as the departure from normality is not extreme. Finally, the input data should be independent of each other, if this is not true, and they are dependent this will lead to inflated PCC values. In terms of what the PCC can reflect about hyperscanning interactions, it can only reflect linear relationships between input data, cannot display any directional information about the relationship and is a bivariate method and therefore other variables cannot be included in the analysis such as systemic confounds, other brain regions or behavioural parameters. Generally the PCC is able to be used with any modality, however its suitability to each method varies slightly. M/EEG analysis focuses highly on analysis of different frequency bands, exploiting the direct relation between neuronal activity and the recording and the high temporal resolution of M/EEG systems, however since the PCC is generally a time domain method it is unable to probe relationships between frequency bands of different participants. Frequency analysis can be conducted by first computing the power of different frequency bands and correlating the power of bands, however this loses the temporal resolution that EEG offers and so the PCC may have limited use in EEG analysis. It's application to fNIRS and fMRI is influenced on how systemic noise is managed during the pre-processing stage. Since there's no ability for the method to separate systemic noise in the frequency domain, mismanagement of systemic noise may cause the PCC to reflect simple systemic increases in both participants rather than neuronal activation specifically if the task-frequency is closely related to systemic component frequencies. However, of the studies reviewed the PCC was applied to EEG (Cassioli and Balconi, 2022), fMRI (Koike et al., 2016; Abe et al., 2019; ;Koike and Sumiya, 2019 Xie et al., 2020; Miyata et al., 2021; Salazar et al., 2021) and fNIRS (Duan et al., 2015; Balconi and Vanutelli, 2017; Balconi and Vanutelli, 2017; Zhao et al., 2017; Balconi et al. 2018b; Fishburn et al., 2018; Dai et al., 2018; Fronda and Balconi, 2020; Hoyniak et al., 2021; Yang et al., 2021; Cheng et al., 2022; Cheng et al. 2022).

5.1.2. Cross correlation

The cross-correlation is an adaptation of the PCC in that the data input is altered such that one variable is time-lagged relative to the other. As such this method also examines how two variables co-vary together. The rationale differs slightly in that it is focused on examining how variables co-vary, when one precedes the other. Applied to hyperscanning this may translate as, if one participant displays a specific action before the other, the cross-correlation can be used to examine how/if the neural activity when that action was carried out, relates to the neural activity of the observer of the action. The assumptions of the data being input are the same as the PCC since the underlying method is the same, it's the input data that varies and is typically applied to time-domain data. With respect to what the method can reflect, it is similar to the PCC. Only linear relationships are unveiled, and other variables cannot be included in the analysis (bivariate), however the

Table 6
List of computational methods of IBC and corresponding studies and modality used.

Method	Modality and Studies
Pearson Correlation (section 5.1.1)	fMRI: Koike et al. (2016); Abe et al. (2019), Koike and Sumiya (2019), Xie et al. (2020), Miyata et al. (2021), Salazar et al. (2021), Ellingsen et al. (2022) fNIRS: Duan et al. (2015), Balconi and Vanutelli (2017), Balconi and Vanutelli (2017), Zhao et al. (2017), Balconi et al. (2018b), Fishburn et al. (2018), Dai et al. (2018), Fronda and Balconi (2020), Yang et al. (2021), Cheng et al. (2022), Cheng et al. (2022) EEG: Cassioli and Balconi (2022)
Cross Correlation (section 5.1.2)	fMRI: King-Casas et al. (2005), Bilek et al. (2015), Špiláková et al. (2020), Ratliff et al. (2021) fNIRS: Azhari et al. (2021), Liu et al. (2021), Lu et al. (2022) EEG: Khalil et al. (2022)
Partial Correlation (Section 5.1.3)	fNIRS: Balconi et al. (2018), Balconi and Fronda (2020b), Balconi et al. (2020), Balconi et al. (2021) EEG: Balconi and Vanutelli (2018b), Balconi et al. (2018a), Balconi et al. (2019, 2020), Balconi and Fronda (2020a, 2020c), Balconi et al. (2020), Balconi et al. (2022)
Spearmans Rank Correlation (Section 5.1.4)	fNIRS: Akimoto et al., 2021, Oku et al. (2022) EEG: Kinreich et al. (2017) MEG: Hasegawa et al. (2016)
Beta Series Correlation (Section 5.1.5)	fMRI: Koike and Tanabe (2019), Yoshioka et al. (2021)
Dynamic Time Warping (Section 5.1.6)	fNIRS: Azhari et al. (2019)
Amplitude Envelope Correlation (section 5.1.7)	EEG: Zamm et al., 2021
General Linear Model (GLM) Classification (Section 5.2.1)	fMRI: Anders et al. (2011)
Cross Brain GLM (Section 5.2.2)	fMRI: Spiegelhalder et al. (2014), Špiláková et al. (2019) fNIRS: Liu et al. (2017), Barreto et al. (2021), Cañigueral et al. (2021), Pinti et al. (2021)
Psychophysiological Interactions (PPI) (Section 5.2.3)	fNIRS: Koide and Shimada (2018)
Wavelet Transform Coherence (Section 5.3.1)	fNIRS: Cui et al. (2012), Dommer et al. (2012), Holper et al. (2012), Cheng et al. (2015), Jiang et al. (2015), Osaka et al. (2015), Baker et al. (2016), Liu et al. (2016), Nozawa et al. (2016, 2019), Tang et al. (2016, 2020), Hirsch et al. (2017, 2018, 2021, 2022), Ikeda et al. (2017), Pan et al. (2017, 2018), Piva et al. (2017), Zhang et al. (2017), Zhang et al. (2017), Dai et al. (2018), Reindl et al. (2018), İşbilir (2016) Xue et al. (2018), Zhang et al. (2018), Balconi et al. (2019), Cheng et al. (2019); Liu et al. (2019), Lu and Hao (2019), Lu et al. (2019, 2021), Lu et al. (2019), Mayseless et al. (2019), Miller et al. (2019); Wang et al. (2019); Liu et al. (2019); Chen et al. (2020); Descorbeth et al. (2020); Dravida et al. (2020); Duan et al. (2020); Li et al. (2020); Lu, Teng and Hao (2020); Lu, Yu and Hao (2020); Nguyen et al. (2020); Noah et al. (2020); Pan and Dikker (2020);, Pan and Guyon (2020); Wang et al. (2020); Sun et al.(2020, 2021); Li (2020, 2021); Zhang et al. (2020); Zhang, Jia and Zheng (2020); Wang et al. (2020); Gamliel et al. (2021); Kruppa et al. (2021); Long et al. (2021); Léné et al. (2021); Zhang et al. (2021); Zhang et al. (2021) Nguyen, Hoehl and Vrtička (2021); Nguyen, Schleihauf, Kayhan, et al. (2021); Nguyen, Schleihauf, Kungl, et al. (2021); Li et al. (2021); Zhang et al. (2021); Wu et al. (2021); Zhang, Jia and Wang (2021); Zhao et al. (2021, 2022); Zhao, Zhu and Hu (2021); Zhu et al. (2022); Pan, Cheng and Hu (2022); Park, Shin and Jeong (2022); Guglielmini et al. (2022); Yuan et al. (2022) EEG: (Stevens and Galloway, 2022)
Fourier Transform Coherence (section 5.3.1)	fMRI: (Stolk et al., 2014; Wang et al., 2022) EEG: (Filho et al., 2016; Balconi and Vanutelli, 2018a; Coomans et al., 2021; Richard et al., 2021) MEG: (Zhdanov et al., 2015)
Total Interdependence (section 5.3.2)	EEG: (Dikker et al., 2017; Chabin et al., 2022)
Imaginary Part of Coherence (section 5.3.3)	EEG: (Dikker et al., 2021)
Partial Wavelet Coherence (section 5.3.4)	fNIRS: (Zhou, Long and Lu, 2021)
Mutual Coherence (section 5.3.5)	fMRI: (Goelman et al., 2019)
Phase Locking Value (section 5.4.1)	EEG: (Dumas et al., 2010, 2012; Yun, Watanabe and Shimojo, 2012; Mu, Guo and Han, 2016; Jahng et al., 2017; Mu, Han and Gelfand, 2017; Pérez, Carreiras and Duñabeitia, 2017; Hu et al., 2018; Barraza, Pérez and Rodríguez, 2020; Dodel, Tognoli and Kelso, 2020; Djalovski et al., 2021; Gumilar et al., 2021; J. Li et al., 2021; Peng et al., 2021; Shehata et al., 2021; Chen et al., 2022; Deng et al., 2022, 2022; Gugnowska et al., 2022; Kang et al., 2022)
Interbrain Phase Coherence (section 5.4.2)	EEG: (Lindenberger et al., 2009; Sänger, Müller and Lindenberger, 2012; Szymanski et al., 2017; Müller and Lindenberger, 2022)
Integrative Coupling Index (section 5.4.3)	EEG: (Müller, Sänger and Lindenberger, 2013, 2018; Sänger, Müller and Lindenberger, 2013; Müller and Lindenberger, 2019)
Phase Synchronization Index (section 5.4.4)	EEG: (Kawasaki, Kitajo and Yamaguchi, 2018; Shiraishi and Shimada, 2021)
Circular Correlation Coefficient (section 5.4.5)	EEG: (Goldstein et al., 2018; Pérez et al., 2019; Zhou et al., 2021; Key et al., 2022; Zivan et al. (2022))
Bispectral Analysis (section 5.4.6)	EEG: (Cha and Lee, 2019)
Weighted Phase Lag Index (section 5.4.7)	EEG: (Ahn et al., 2018)
Granger Causality (section 5.5.1)	fNIRS: (Ono et al., 2021)
Conditional Granger Causality (section 5.5.1)	EEG: (Sciaraffa et al., 2021)
Phase Slope Index (section 5.5.2)	EEG: (Fenwick et al., 2019)
Partial Directed Coherence (section 5.5.3)	EEG: (Astolfi et al., 2010, 2011; Fallani et al., 2010; Toppi et al., 2016; Sciaraffa et al., 2017; Ciaramidaro et al., 2018; Santamaria et al., 2020)
Unspecified correlation (section 5.1)	fMRI: (Krueger et al., 2007; Saito et al., 2010; Shaw et al., 2018) fNIRS: (Holper et al., 2013; Hoyniak et al., 2021)

implementation of a time-lag of one variable relative to the other allows for a degree of asymmetry in the analysis. If the correlation is high when one participants data is lagged relative to the other, but not if the reverse is done, it implies that in the first case the lagged participant has some (loose) predictive relation to the other participant. Cross-correlation favours higher temporal resolutions (compared with PCC) since more time points allows a more granular way to evaluate time periods of interest. However as discussed above M/EEG data typically focuses on specific frequencies, and not purely on the time domain data. As such this form of correlation may favour fNIRS analysis, with the contingent the systemic components are adequately filtered. The cross correlation was applied to EEG (Khalil et al. 2022), fNIRS (Azhari et al. 2021; Liu et al., 2021; Lu et al., 2022) and fMRI (King-Casas et al., 2005; Bilek et al., 2015; Špiláková et al., 2020).

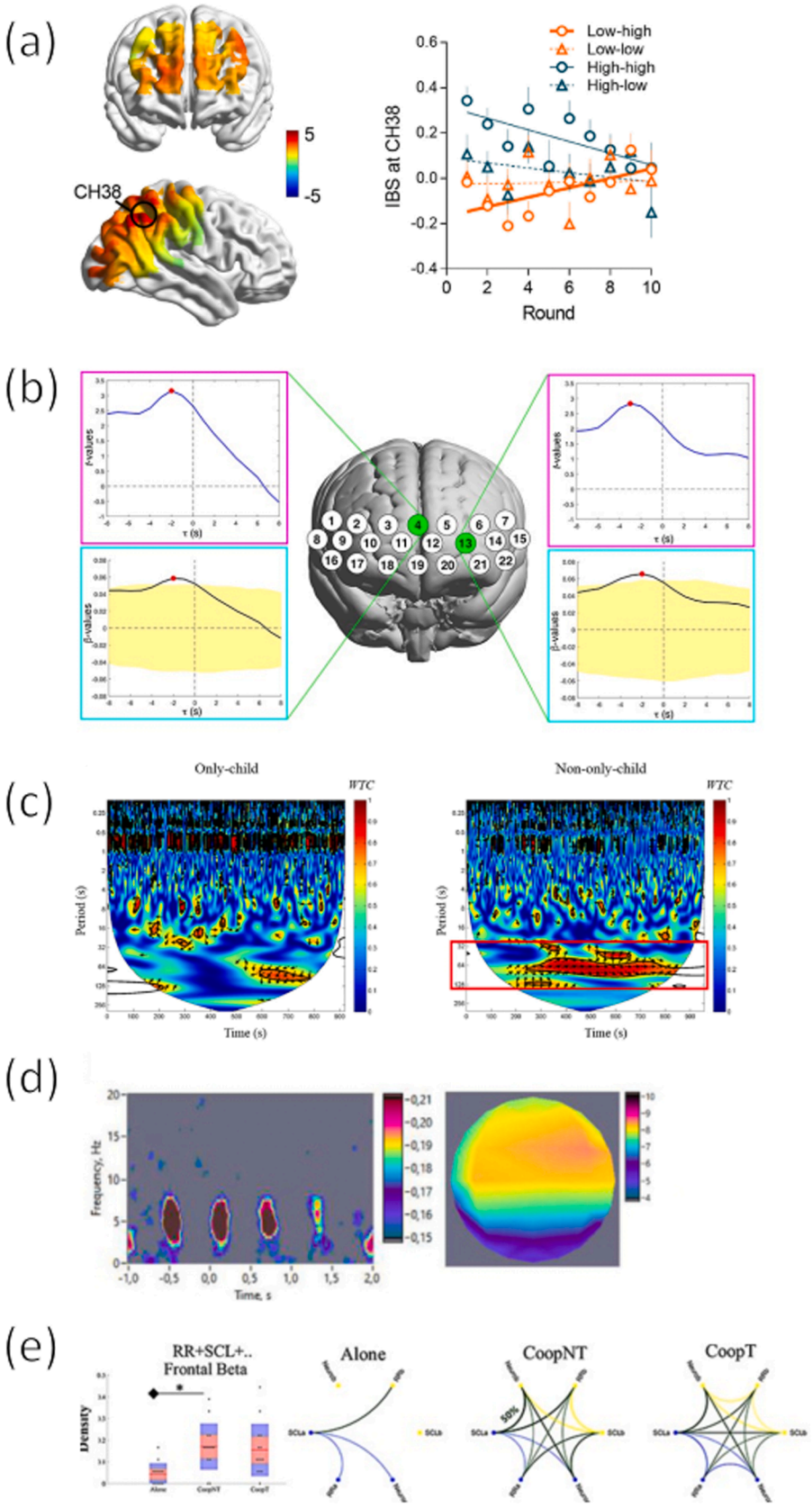

Fig. 5. Examples of how hyperscanning metrics can be represented for each of the analytic categories in this review. (a) is an example of Pearson correlation data from (Cheng et al., 2022), the left hand side shows t-value maps of correlation values from a dyad. (b) represents the cross brain GLM results from (Pinti et al., 2021), the upper boxes show t-values at different time lags, whilst the bottom show beta values at different time lags. (c) shows wavelet coherence spectrograms of fNIRS data from a channel of a dyad from the study by (Wu et al., 2021). (d) shows the inter-brain phase coherence from (Muller and Lindenberger., 2022) showing both the time-frequency representation of the data and the topological distributions of the strength of interbrain phase coherenc€(e) Is the representation of multi-variate Granger causality from (Sciaraffa et al., 2021) where the connections on the right hand side in green represent the between brain connectivity and the thickness represents how many dyads had that connectivity. The plot on the left shows the density of between subject connections.

5.1.3. Partial correlation

The Partial Correlation also observes how input variables co-vary, with the output value explaining whether they are related to each other in a linear way. This form of correlation varies with respect to the previous two in that it isolates the relationship between two input variables whilst controlling for a third confounding variable. With respect to hyperscanning this can be used to compute the correlation between neural signals from two participants whilst controlling for some confound which would cause inflated correlation values. The assumptions of the input data are the same as for PCC, however this form of correlation is a multivariate method, allowing the inclusion of confounding variables to be accounted for. However, similarly to the PCC it is only able to reflect linear, symmetric relationships between input data which is also usually in the time-domain. Since this allows the inclusion of multiple variables, it is beneficial to be used in cases where multimodal data can be acquired, such as physiological information or behavioural parameters, which can account for any inflated correlations caused by systemic influences on the neuronal data, or artefacts linked to specific behaviours. Furthermore, high spatial resolutions may allow for interesting analyses whereby regions which are physically connected to another can be exempted from the correlation analysis. For example, if region A in participant 1 is influenced by region B, computing the correlation between region A participant 1 and region C on participant 2 may give the same correlation as computing region B on participant 1 and region C on participant 2 as the regions A and B are not independent of each other. This method was used by 12 studies from the same group, 8 of these (Balconi and Vanutelli, 2018b; Balconi et al. 2018a; Balconi et al., 2019, 2020; Balconi and Fronda, 2020a, 2020c; Balconi et al. 2020; Balconi et al. 2022) used EEG data, whilst 4 (Balconi et al. 2018; Balconi and Fronda, 2020b; Balconi et al. 2020; Balconi et al. 2021) used fNIRS, the application is the same for both. The formula used by the these studies is provided in the supplementary materials Eq. S2.

5.1.4. Spearman rank order correlation

The output of the Spearmans Rank Correlation is based on the sum of squared differences between the rank of the input data. Therefore the input values must first be ranked in some form before computing the correlation between them with the output reflecting the ordinal relationship between data. The rationale of the method is understood in comparison to the PCC. The Spearman correlation can reflect non-linear, monotonic relationships whilst also being more robust to outliers in input variables, and non-normally distributed data. The main draw of using the Spearmans rank correlation as opposed to other forms, is in its ability to reflect non-linear relationships between the ordinal input data. However, as expected an important assumption of the method is that the data is ordinal. As such the neuronal data being used must be ranked in some way before computing the Spearman correlation. There are no specific parameters of the method which increase its suitability aside from what has already been discussed about other correlation forms. However, how the data is ranked is important and should be clarified by authors; (Hasegawa et al., 2016; Kinreich et al., 2017) using EEG and MEG respectively, ranked the frequency components of their neural data, whilst (Akimoto et al., 2021) using fNIRS did not specify the ranking of their data.

5.1.5. Beta series correlation

The Beta Series Correlation is a form of analysis based on the 'Beta Series' form of analysis developed by (Rissman et al. 2004). The rationale for the Beta series as specified by the authors of the method is such that events occurring within a short time frame cannot be specifically disentangled due to the slow HRF. A typical analysis models each task which may consist of multiple events; the Beta series method models each event with separate regressors such that a time-series of beta values can be obtained. The application of this to hyperscanning is conducted for the same reason – the HRF may overlook individual transient events and so modelling all events of interest as separate regressors may offer a higher-resolution view of the interaction. This is done for both participants and then the outputs are correlated. The assumptions of this method depend on (1) the form of correlation used, and (2) the General Linear Model (GLM) framework, which are broadly the same as other forms of correlation with the addition of predictor variables not having multicollinearity between them. In terms of what can be evaluated using this method, it depends mainly on what form of correlation is applied to the resultant beta-series. The authors using this method (Abe, et al., 2019; Yoshioka et al., 2021) did not specify which form of correlation they used. The use of this method is mainly focused upon modalities exploiting the haemodynamic response to stimuli since it is aimed at overcoming the slowness of HRF modelled data. However as of writing it has only been applied to fMRI data.

5.1.6. Dynamic time warping

Dynamic Time Warping (DTW) is an algorithm used to assess similarity between input data by measuring the distance between input data. The rationale behind its use is that traditional means of measuring similarity typically assumes a one-to-one matching, which may not be true if data are similar but originate from different sources (for example, two people walking with different speeds). The DTW provides a means to assess similarities independent of durations, timings or other factors influencing the temporal dynamics of the originating system. It's normal use outputs a distance index which signifies how closely matching one time-series is to another. The use of DTW in hyperscanning follows much the same method; the output distance index is used as a metric of 'synchronization' between participants. There are a few assumptions when using the DTW, the first being the start and end points of both input data are the same (one time series does not extend further than the other), data is monotonic, that corresponding points in both time series are likely to be close together independent of temporal distortions, and the warping path (from which the distance index is computed) exhibits continuity to prevent illogical jumps forward. This is a bivariate method, however the linearity and symmetry depends on the distance metric used. Azhari et al. (2019) used Euclidean distance as the distance metric, however other metrics may be used although care should be taken to ensure that the distance metric represents the underlying relationship adequately to provide meaningful results. Its suitability is focused towards higher temporal resolution data because it matches the data points of one participant to the data points of another, if there are too few the algorithm may not reflect useful information. In any case the method has only been applied to fNIRS data, although its use with EEG may be interesting.

5.1.7. Amplitude envelope correlation

The Amplitude Envelope Correlation refers to the correlation of the envelope of signals. The correlation method was unspecified, but essentially the method reflects the covariance of the envelope of neuronal data. The rationale of this is specifically aimed at neuronal data, as the original application was to assess coupling between regions using EEG data (Bruns et al., 2000). The authors of the method state the gamma band synchronization has been found between regions in the animal brain, where the scale of distances between ROI is millimeter, however this is rarely reported in humans. They propose that the longer distances may introduce variations in the phase of activation, which prevents coupling from being detected using coherence. They propose to use the correlation between the envelope of the amplitude of EEG signals instead because it allows for more 'temporal jitter' than coherence because the envelope of the band-limited signal does not change as rapidly as the signal themselves. Its application to hyperscanning by Zamm et al., 2021 using EEG data was based around a similar rationale – they sought to evaluate synchrony between data independent of phase coherence. Similar to DTW and Beta series correlation, the assumption surrounding the correlation are the same as the PCC since this is the correlation used by Bruns et al. (2000). Further, the computation of the amplitude envelope was done using the Hilbert transform which

requires the signal for which the envelope is computed to be narrow-band (requiring the EEG data first be filtered to the frequency band of interest), free from noise and with no phase distortion. As with the PCC the method can show the linear, symmetric relationship for the bivariate inputs. The method was originally developed to examine high frequency coupling between brain regions and so favours higher temporal resolution data, especially since the envelope requires a higher number of data points to represent a meaningful evolution of neural data over time.

5.2. Regression

Closely related to correlation are regression techniques. All methods in this section stem from the General Linear Model (GLM). The GLM is a linear regression technique which essentially computes the similarity between modelled variables (also called predictor variables or regressors) and the measured data, reflected in a regression coefficient (Eq. S3 in supplementary materials).

5.2.1. GLM classification

This method, as applied by Anders et al. (2011), uses the Euclidean distance between the mean regression coefficient of one participants emotion-specific-network and a voxel from the other participant to evaluate whether the emotional response of one person elicits emotion-based activation in the other. Essentially the rationale behind it is, if there is a small distance between the regression coefficients of both participants then it's likely that there is an interaction between the two participants. The assumptions of this method are those of the GLM in general. This requires the residuals of the model are normally distributed, predictor variables are not colinear, and data is homoscedastic. Alongside these assumptions, the GLM can only reflect the linear relationship between the predictor variables and the measured data. However, the implementation of the GLM in this method allows asymmetric relationships to be evaluated, since the distance is based on the emotion-specific-network of one participant to the other, which may not be true in the reverse case. GLM based methods are more suited to haemodynamic based modalities since it is the standard analysis method for single brain functional activaton. Additionally, the HRF can be modelled as a canonical response to stimuli, whilst there is no established canonical response to stimuli for M/EEG data. Anders et al. (2011) used this method with fMRI data makes good use of the spatial resolution of fMRI by computing emotion-specific-networks based on high resolution neural data.

5.2.2. Cross brain GLM

This implementation of the GLM uses neural data from participant B as the predictor variable for the neural response of participant A, using the output regression coefficient as the determinant of increased IBC in specific experimental conditions. This was further extended by introducing a time-lag to one participants data by (Spiegelhalder et al., 2014; Špiláková et al., 2019; Pinti et al., 2021) using fMRI and fNIRS to evaluate lead-lag relationships between participants (Eq. S4). Liu et al. (2017) regressed fNIRS data from one participant onto the data of the other and included the task-timings as an additional regressor. Barreto et al. (2021) tested both support vector and ordinary least squares using fNIRS data in their ability to predict the signal from one participant based on the other. They obtained regression coefficients by computing the regression between homologous channels of partnered participants. The coefficients where then used to compute the predicted signal of one participant, and the correlation between predicted and real signals used to evaluate performance of each method. Cañigueral et al. (2021) used a multivariate GLM approach with fNIRS data, eye-gaze and facial motion from both participants and the brain activity from participant B in the model which was used to predict the brain activity of participant A. Evidently this is a widely versatile method to evaluate IBC, able to evaluate lead-lag relationships, incorporate multivariate data and to predict neural response based on partner data. The detection of lead-lag relationships is suited to higher temporal resolutions for the same reasons as cross-correlation is, whilst predicting data from one participant based on another may be more suited to higher spatial resolution as more localized neural responses can be used as the basis of prediction. Additionally, this method does not require a canonical response as the predictor variable since the neural response of the partner is used as the predictor variable.

5.2.3. Psychophysiological interaction (PPI)

The implementation of of PPI to fNIRS hyperscanning by Koide and Shimada (2018) follows the same rationale and metric of IBC as the previous GLM based methods. However, PPI analysis (Friston et al., 1997) was developed to evaluate functional networks with 2 extra predictor variables to remove spurious connections, whilst the third regressor is the seed-region for which connectivity to is desired two (see O'Reilly et al., 2012 for detail). In the case of hyperscanning (Koide and Shimada, 2018) used the channel of the partner showing the peak activation during the task as the seed-region.

5.3. Coherence

In general, coherence-based methods are analogous to computing the correlation of time-series data, however the data is represented in the frequency, or time-frequency domains. For a comparison of coherence and correlation using EEG data see (Guevara and Corsi-Cabrera, 1996). The first stage in a coherence based method is the conversion from the time-domain to the frequency/time-frequency domain. This is done using either the wavelet or Fourier transform (WT/FT).

The FT uses sine and cosine waves with varying frequencies as basis functions to determine frequency content of a specific period of time-series data, normally a pre-defined window which is slid over the entire time-series which are then averaged (for example, Welch (1967)) in this way the FT of a time-series has good spectral resolution but poor temporal resolution; you may know that a frequency exists in the signal, but not at what time this occurs. In comparison, the wavelet transform computes the frequency content using 'wavelets' as basis functions, which are varied in size (for a full explanation of wavelet analysis see (; Torrence and Compo, 1998; Chang and Glover, 2010)). Wavelet analysis is able to provide good spectral and temporal resolution, providing the power of specific frequencies at each time point. The instantaneous information makes it better suited to non-stationary signals such as those arising from physiological processes.

All of the methods in this category use the magnitude squared coherence (MSC) in their computation of IBC. First the spectral content of the two signals is determined and then the cross-spectral density (Eq. S5) of the input signals are computed. Using this the MSC (Eq. S6) is computed. The MSC computed using wavelet transformations is often referred to as the wavelet transform coherence (WTC) and the MSC when using Fourier transformations, however the two are the same, only the method to obtain frequency/time-frequency information differs. 7 methods were discovered in the coherence category: Fourier Transform Coherence, Wavelet Transform Coherence, Total Interdependence, Imaginary Part of Coherence, Partial Wavelet Coherence and Mutual Coherence.

5.3.1. Fourier transform coherence

The FTC computes the common strength of specific frequencies of a signal, operating exclusively in the frequency domain. The rationale, and power, of this method is that it is able to identify specific frequency components which are common to both signals, which may be covered when conducting time-series analysis exclusive in the time domain. Applying this to hyperscanning (and neuroscience in general) is that different frequencies in the neural data correspond to different neural functions, this is especially true with direct measures of brain activity (M/EEG) but also important with indirect measures of activity since the

different components represent different physiological properties (not specifically neural). Evaluating the coherence of different frequencies of interacting participants may be indicative of underlying common phenomena. The assumptions of this method mainly lie with the conversion to the frequency domain. To ensure meaningful interpretations users must ensure the data is free from noise and is adequately sampled to reflect the underlying brain function. Additionally, Fourier transforming data assumes data is stationary such that the frequency content is consistent over time. This is often not true with physiological data in general (fNIRS data is a clear example) and leads to the issue of uncertainty in where frequency components lie within the time data. As was the case with PCC the FTC is only able to reflect linear and symmetric relationships for bivariate data. The power of FTC (coherence in general) is to investigate the frequency components of the data, as such it is suited to high temporal resolution data which can reflect the different frequency components that make up the underlying brain function. The FTC was used by 7 studies; (Filho et al., 2016; Balconi and Vanutelli, 2018a; Coomans et al., 2021; Richard et al., 2021) used EEG, (Montague et al., 2002; Saito et al., 2010) used fMRI and (Zhdanov et al., 2015) used MEG.

5.3.2. Wavelet transform coherence

Similar to FTC, the WTC also computes the common strength of specific frequencies of a signal, however it does so in the time-frequency domain. The rationale extends beyond the FTC since the WTC can unveil frequency information throughout the duration of the signal with decreasing time resolution as the frequency gets lower. This is specifically of use for physiological data since the frequency content varies over time (most biological signals are non-stationary). As the method is sensitive to the power in a signal (and not the phase of the signal), it is capable of capturing out-of-phase relationships between brain activity in participant A and participant B, unlike simple correlation methods. This means it has more flexibility to indicate interactions where A and B are imperfectly related to one another. When using the WTC users must ensure that the underlying wavelet function (used to compute spectral content of the signal) adequately represents the original signal (Zhang et al., 2020). Data should also be clean of artefacts so the power of each frequency represents neuronally relevant phenomena and not commonly occurring systemic changes, or noise. The method is only able to reflect the linear relationship between one location on one participant and one on another, and the output is symmetric. The WTC is suited to modalities which are able to reflect underlying frequency components adequately. Where the FTC can only interrogate specific frequency components commonly occurring at a single time, the WTC is able to interrogate how the co-occurrence of individual frequency components evolves over time. This is an important distinction between the two methods, and grants the WTC superior power to interrogate social interactions and how they evolve and manifest over time. Additionally, since the WTC is typically computed between analogous locations of interacting participants it favours a higher spatial resolution in order to accurately and meaningfully reflect commonly occurring frequencies. If the activity of one person is incorrectly spread across multiple regions (via volume conduction for example) this may manifest as multiple areas showing falsely high WTC with correspond locations in the partner. The WTC is the most commonly used method in the literature, used by 91 studies of which 1 was EEG (Stevens and Galloway, 2022) and the rest fNIRS.

5.3.3. Total interdependence (TI)

Two studies using EEG used the Total Interdependence (TI) to compute IBC (Dikker et al., 2017; Chabin et al., 2022). This was developed by Gel'fand (1959) and adapted for fMRI signals by Wen et al. (2012) to investigate resting state functional connectivity. The method infers IBC by summing all possible feedback between the time-series, computed in the frequency domain. Feedback in this case is used in the Granger sense such that for two time-series, X and Y, if the past of Y can be used to improve the prediction of X more than using the past of X by itself, then Y is said to Granger cause X. Therefore in this case the TI is considered as the sum of linear feedback from X to Y, linear feedback from Y to X and instantaneous linear feedback (Geweke, 1982). The rationale of the method applied to hyperscanning is that traditional measures (such as coherence and correlation) do not take into account dependence beyond contemporaneously acquired data points and the use of TI provides a wider picture of all forms of interaction and dependence between participants. The assumptions for the method depend mainly on how the spectral information is computed using either the Fourier or Wavelet transforms. The formula to compute the TI provided by Dikker et al. (2017) (Eq. S7) allows the TI to be interpreted as the total amount of mutual information between two Gaussian stationary processes. Necessarily then, TI makes an assumption that the signals being investigated are Gaussian stationary (Wen et al. (2012), for long epochs of EEG data this is not strictly true. However, since (Dikker et al., 2017) computed the TI for smaller epochs it can be considered approximately Gaussian stationary. However care should be taken to ensure that this assumption is true for the users data when using the TI. Since the method sums all the feedbacks between the two signals the output is therefore a symmetric measure, reflecting the linear relationship of two variables.

5.3.4. Imaginary part of coherence (ImC)

The coherence (not the MSC) is a complex valued number, where the imaginary part represents the phase relationship between the input data. This method uses that imaginary part to determine IBC. The original method developed by Nolte et al. (2004) was based on the idea that volume conduction can cause the activity of a single anatomical location to be measured in multiple EEG channels. Volume conducted activity should have synchronous phase, which can be identified and used to only consider real EEG activity. The application of this method to the one EEG study that used it (Dikker et al., 2021) follows a similar rationale; the environment they acquired the data was heavily influenced by noise induced in the EEG system from the environment, which manifests as common signals with 0 phase difference and so the ImC is able to account for this and evaluate IBC from participants in the noisy environment. The assumptions behind the computation depend again on the method of computing the frequency composition of the signal and the output reflects the symmetric linear relationship between two input variables. The method is suitable for any modality since the imaginary component can be acquired however its usefulness is generally focused around its application to EEG data since it suffers from volume conduction and electrical interference.

5.3.5. Partial wavelet coherence (pWTC)

The underlying metric inferring IBC of the pWTC is the same as the WTC however it includes the ability to control for an additional variable, analogous to the Partial Correlation. The original authors of the method (Mihanović et al. 2009) developed it to compute the impact of tidal flow on other geographical parameters, whilst disentangling confounding effects. This was then applied to fNIRS data by Zhou et al. (2021). They used it to control for the autocorrelated nature of fNIRS data which can lead to inflated coherence results if not dealt with adequately. In this case the authors included the auto-coherence of one participant, the contemporaneous coherence between participants and the time-lagged coherence of one participant to the other (Eq. S9). The assumptions behind the computation of the pWTC remain the same as for the WTC. In contrast to the WTC, the inclusion of the time-lagged coherence means that there is an asymmetric nature to the output, and it can be used to assess some causal nature of the interaction, the authors compared its causal output to Granger causality, with the two providing comparable results. In addition, although the authors of this hyperscanning study used it control for the autocoherence of one participants data, it can feasibly be used to control for the coherence of some other datasets, for example the coherence between breathing rate and fNIRS of one

participant, to control for any systemic contamination associated with the fNIRS data. Although only used for fNIRS data, the method could be applied to EEG to control for volume conduction, or to fMRI controlling for specific anatomical locations which may be dependent on another location.

5.3.6. Mutual coherence (MC)

The MC was developed by Goelman and Dan (2017) fMRI by adapting the WTC to detect directional functional connectivity between brain regions by quantitatively evaluating the phase delays between brain regions (Eqs. S10–S13c). As such it computes the common strength of specific frequencies, as standard with the WTC but also incorporates the phase relation between inputs to provide a directional, hierarchical evaluation of the inputs. The rationale of the original method as stated by the authors is that the non linearity of the method allows multiple nodes to be considered when looking for functional connectivity between multiple regions, and the phase relationship between each region allows directed functional connectivity to be assessed. The extension of this rationale to hyperscanning is to assess directed inter-brain functional connectivity, to determine which seed-region in one participant influences regions in the other (Goelman et al., 2019). This method reflects the asymmetric, non-linear relationship between multiple variables. The authors of the method state that it is suitable to be applied to wide range of modalities (and fields of study), however there is a benefit in using it with modalities with higher spatial resolution (such as fMRI as it was developed for) since it provides interesting information about the networks of social function and the directions of operation.

5.4. Phase synchrony

Phase synchrony methods base IBC on whether a phase relation exists between input data. All of the studies using this category of methods used EEG (Ahn et al. (2018) used EEG and MEG) as the imaging modality. The high temporal resolution of EEG allows the phase dynamics of the signal to be better interrogated since more datapoints are acquired from the recording location which can be used to determine the phase. 7 methods were found for this category: Phase Locking Value, Interbrain Phase Coherence, Integrative Coupling Index, Phase Synchronization Index, Circular Correlation Coefficient, Bispectral Analysis and Weighted Phase Lag Index.

5.4.1. Phase locking value (PLV)

The most common method within this category is the PLV, used by 20 studies. The PLV was developed by Lachaux et al. (1999) to evaluate functional connectivity between EEG channels and measures the inter-trial variability of the phase difference between two signals (Eq. S14). If two signals are consistently phase locked throughout the experiment, they will exhibit a high PLV value. The rationale of the method is that phase locking must occur between interacting regions for the signal to reach the scalp, if the phases where distributed broadly they would annihilate and be undetectable. They also provide reasoning to use the PLV compared to the coherence: (1) coherence requires stationary data (2) coherence does not consider phase relation and phase vs amplitude relation is unclear. Although the first point does not hold much relevance when using the wavelet transform to obtain phase, the second point is still true, and applies also the its use with hyperscanning. Conceptually, if a researcher is using coherence to investigate IBC, and they find high coherence and thus conclude increasing IBC and then repeat the study with the PLV as their metric of IBC, but find low PLV, combining the two interpretations is challenging. Lachaux et al. (1999) argue that the PLV is enough to determine interaction and that there is no clear interpretation for changes in coherence beyond obvious interdependency. When computing the PLV the main assumptions are that the instantaneous phase values are obtainable (with the method of obtaining them (either wavelet or Hilbert transform) carrying its own assumptions) and the phase values reflect the underlying dynamics adequately. The method can only display the linear symmetric relationship between inputs and is only suited to bivariate data. The application of the PLV to hyperscanning has only been carried out with EEG data. EEG data is suited to its use due to its high temporal resolution which is able to reflect the underlying neural oscillations well.

5.4.2. Interbrain phase coherence (IPC)

The IPC was used by Lindenberger et al. (2009), Sänger et al. (2012), Szymanski et al. (2017), Müller and Lindenberger (2022). The method bares a very close resemblance to the PLV, and the formula is in effect the same. In some cases the method is also called the Phase Locking Index (PLI). The key distinction is that the PLV computes the phase difference for each time point in a trial and averages all the phase differences within a trial. In comparison the IPC computes the phase difference based on a whole trial. Burgess (2013) discuss the differences between the two in more detail. The assumptions, rationale and suitability of the method are the same as the PLV.

5.4.3. Integrative coupling index (ICI)

The IPC/PLI was additionally used by Müller et al. (2013, 2018), Sänger et al. (2013), Müller and Lindenberger (2019) to compute the ICI. Phase stability values are first obtained using the IPC (or as the authors now call it, the Phase Synchronization Index). The number of phase locked points are counted between specific bounds (positively or negatively coupled points and the sum of the two, Eq. S15a-S16)). The method is adapted from the global lability of synchronization method from Kitzbichler et al. (2009). They propose that the method is able to provide a global metric of the extent of synchronization in a system, which allows the user to ascertain how long phase differences remain stable within defined phase difference boundaries. Extending this to hyperscanning and two neural signals, the authors of the method state that this is a directed measure of phase synchrony, indicating the relative extent of positive phase synchronization and can provide phase synchronization with more specificity. As the main determination of IBC is still really the PLI/PSI/IPC the mathematical assumptions and suitability around the IPC are the same as those methods.

5.4.4. Phase synchronization index

Kawasaki et al. (2018), Shiraishi and Shimada (2021) used the Phase Synchronization Index (PSI) method, which is different to the PSI/-PLI/IPC method used for the computation of the ICI. The origin of the method is unclear, and the authors do not state any rationale to using this over other methods evaluating phase synchrony. The method measures the phase invariance in a specific time window between two channels, (Eq. S17).

5.4.5. Circular correlation coefficient (CCor)

Computing the PCC of circular data (such as phase data) is not mathematically correct because the data wraps around and leads to uninterpretable results. The CCor method was developed to account for this, and its output is based on the circular covariance of differences between the observed and mean phase (Eq. S18) (Jammalamadaka, Sengupta and SenGupta, 1999; Burgess, 2013). The rationale for hyperscanning follows the same reasoning; computing the correlation of phase values requires the use of circular statistics and this was used by Goldstein et al. (2018), Pérez et al. (2019), Zhou et al. (2021), Key et al. (2022), Zivan et al. (2022). How correlated phase values are follows the same essence of phase locking/invariance. To acquire meaningful results the method assumes that the data is circular and the circular distribution is uniform. Again, the suitability of the method really depends on the ability of the modality to obtain meaningful and accurate phase values for the underlying neural dynamics.

5.4.6. Bispectral analysis

The Bispectral Analysis developed by Barnett et al. (1971) measures the non-linear phase coupling between frequency components of an

individual EEG signal (Eq. S19). The rationale of the method is that typical spectra analysis, such as the FT, only investigates whether frequencies exist in a signal, providing no information about how different frequencies may be coupled together. Computing the bispectrum can provide information about this. However, the adaptation of this method to hyperscanning is less clear. Since the original formulation is to investigate different frequency components within a signal, modifications must be made to it to extend it to between signals. How (Cha and Lee, 2019) did this is not stated. Additionally, the interpretation of any output from this method would be difficult to parse since it would investigate how different frequency components of one signal are coupled to different frequency components of the other, outputting a rather large amount of data. Due to the lack of clarity about how the original method was adapted to or applied to hyperscanning data the assumptions and suitability of the method are difficult to ascertain.

5.4.7. *Weighted phase lag index (wPLGI)*

The Phase Lag refers to the asymmetry of the distribution of phase differences of input data; essentially how much lag is there between data. The rationale differs to the previous phase synchrony methods, the original authors (Stam et al., 2007) (Eq.S20) specify that there is difficulty in assessing connectivity between electrodes because volume conduction causes phase to couple around 0° at the souce level, which is likely to not be true phase synchrony. As such, the presence of consistent non-zero phase lags between time-series is not likely to be volume conduction. The method they propose can determine in which direction the lag lays, providing a means of directional evaluation. This was further extended by Vinck et al. (2011) who claimed that small perturbations about 0° can alter the lead/lag relationship between time-series and introducing a weighting factor defined by the magnitude of the imaginary component of the coherence between the time-series can account for this (Eq. S21). Although hyperscanning doesn't suffer from the effects of volume conduction between time-series because they originate from different scalps, the effect can still be apparent if trying to determine spatial localization between participants. If two channels on each participant are effected by volume conduction it will be difficult to differentiate between IBC of those channels on both participants. However, how this method deals with the issue of volume conduction between participants is unclear since they originate from different sources and so it is unlikely they will have consistent zero phase lags anyway. The assumptions of this method again depend on which method is used to determine phase, however it does require the instantaneous phase of each signal and so the wavelet or Hilbert transforms are required.

5.5. *Causality*

Ten studies used some form of Causal analysis to investigate IBC. All of the studies here used EEG aside from Ono et al. (2021) who used fNIRS. All of the methods in this category, except the Phase Slope Index (PSI), are based on the concept of Granger Causality (GC) (Granger, 1969). The concept of GC can be summarized based on two premises: (1) A cause occurs before its effect and (2) Knowledge of the cause improves the prediction of its effect. Three methods claim to assess causal relationships: Granger Causality (and its conditional form), Partial Directed Coherence and Phase Slope Index.

5.5.1. *Granger causality and conditional granger causality*

Granger causality is perhaps the most widely known form of inferring some sense of causality, which it bases on the ratio of the variance of the residuals (error) of two autoregressive models; one including the past of another signal. The rationale from Granger (1969) is, a signal, x, is said to Granger Cause a signal, y, if the past of x improves the prediction of y, compared to using the past of y on its own. The extension of this rationale to hyperscanning is simple, if the information from one participants past (when they acted for example) can be used to better predict the future of the other participant then there is some interaction between them, which is normally denoted as 'Granger-causal relationship', this was the form used by Ono et al. (2021) (Eqs. S22a–S23). This can be extended further to include other vaariables, in a multivariate (or conditional) Granger causality (used by Sciaraffa et al. (2021). The conditional form allows cases where x and y are both dependent on a third signal, z, then some similarity between x and y will exist which may be mistaken as causality by including z in the autoreggresive models (Eq. S24a and b). The use of GC analysis requires the data to not be autocorrelated and the lag which is used should adequately encompass the underlying dynamics being investigated. Since the method is causal it is necessarily asymmetric, and can represent the linear relationship between input data. The conditional form is multivariate, whilst the standard is bivariate. The suitability of the method to fNIRS and fMRI has seen some debate because of the thought that (1) the HRF varies between locations and (2) the delay between the neuronal activity and the HRF response. The first point has been theoretically and with simulations been disproven for fMRI data (although since fMRI and fNIRS interrogate the HRF the reasoning should still apply to fNIRS) (Seth et al., 2013). The second point is an issue since the GC incorporates a time-lag, if this is not chosen correctly, it may infact be including some other non-relevant information from the past of one participant when assessing causality, such that the perceived neural function is either not included, or included with other contaminants (Friston, 2009; Friston et al., 2013). As such the method is well suited to M/EEG data because of its high temporal resolution which reflects direct neuronal activity (Seth et al., 2015). The method has only been applied to fNIRS and EEG data in the hyperscanning literature, likely due to the benefit of high sampling rate from both. However its application to fNIRS should not overlook the fact that the HRF is still not a direct measure of neuronal activity and is subject to the same criticisms as fMRI.

5.5.2. *Partial directed coherence (PDC)*

The concept of Granger causality was extended to the frequency domain by Baccalá and Sameshima (2001) with the PDC. This follows the same logic as the GC, however it uses the frequency domain representation of the multi-variate auto-regressive model coefficients to determine the causality between data (Eqs. S25–27). The rationale for the method was to provide additional causal analysis in the frequency domain, with multi-channel data. The multi-channel aspect provides a powerful means to evaluate directed networks (Baccalá and Sameshima (2001) developed it for within brains). The benefit of applying this to HS are clear, the method essentially combines the benefit of frequency domain analysis, with asymmetric information, with multi-channel data. This can then be used to examine how the entire channel set of one participant interacts with the entire channel set of the other. The assumptions for the input data are that it is free from any confounds which will contaminate frequencies and that the model order is able to accurately capture underlying dynamics. The method has only been evaluated using EEG hyperscanning data, since it heavily requires high temporal resolution (due to the frequency domain representation and the model order requirement) it is likely beneficial to be used with EEG data, although (Burgess, 2013) suggests that the PDC is susceptible to spurious couplings. Some work has been carried out using the PDC for fMRI (Sato et al., 2009) but not with hyperscanning data. The multivariate nature of the method coupled with fMRI high spatial resolution may provide a powerful means of evaluating inter-brain networks, however care should be taken due to the slow temporal resolution of acquisition and slowness of the HRF.

5.5.3. *Phase slope index*

The Phase Slope Index, introduced by Nolte et al. (2008) and applied to hyperscanning by Fenwick et al. (2019), monitors the change in phase difference over time, assuming that if there is a consistent change in the difference, one signal is likely leading the other (Eq. S28). The authors developed this method to account for (unspecified) confounding

background activity which significant spectral properties causing artificial directional flow results between time series. The method further weights phases from different frequencies according to their statistical relevance. This was used by Fenwick et al. (2019) specifically to account for volume conduction, however the same reasoning about volume conduction as discussed in Section 5.4.7. The method is able to reflect non-linear and asymmetric relationships of the input data, for bivariate data. The suitability favours EEG as it requires a high temporal resolution to assess the phase differences, and the coherence in order to weight appropriately.

6. Discussion

A total of 27 different analysis methods (summarized in Table 7) were found in our review to compute the IBC in hyperscanning studies. Overall, it seems that the preference for a given analytic method depends on the neuroimaging modality which in turn determines the properties of the signal. Specifically, fMRI hyperscanning studies favoured correlation based methods, whilst EEG favoured phase synchrony, fNIRS favoured coherence and MEG studies were split between correlation and coherence. The preferences are based on the temporal and spatial specifications of each modality. The preference with respect to the temporal resolution is dependent on a modalities temporal resolution relative to the underlying physiology. For example, the HRF is a slow response, however fNIRS acquires data faster than the HRF, hence it oversamples the underlying neuronal physiology and more accurately reflcting the underlying HRF. Whereas fMRI has a slower acquisition time, with a TR of 2.5 seconds in some cases, which is at the upper limit of reflecting the HRF, as such it may miss more transient information present in the signals. Therefore, since higher temporal resolution can more accurately represent frequency and phasic properties of acquired neuronal signals, modalities which do have a higher temporal resolution favour analytic methods requiring frequency/time-frequency transformations. Causal methods in general may also favour higher temporal resolutions since they rely on using the past data points to make causal interpretations – if there are not enough points in the past the results may be less accurate. In comparison a higher spatial resolution favours regression methods since multiple brain areas can be included in the regression models.

In order to improve the clarity of what hyperscanning studies investigate, and to place these results in the wider scientific context authors should specify their rationale for the use of their chosen analytic method to determine IBC. For example, the two most common methods, the WTC and the PLV, use the power of common frequencies and phase-invariance respectively. However, two signals can have a high common frequency, whilst not phase-locked, and vice versa. The interpretation of the interplay between different metrics and whether they show, or do not show, IBC is unclear. Focusing on methods utilising phase relationships specifically, different measures have different and (sometimes contrasting) views of what should be perceived as 'real' phase synchrony, for example the Phase Lag Index requires asymmetrical phase coupling to perceive IBC, whilst the PLV requires consistent phase coupling and the Phase Slope requires consistent changes to the phase difference over time. Interpreting the underlying neuroscience of these

Table 7
Summary of methods included in this review.

Metric	Domain	Property inferring interbrain coupling	Bi/Multi Variate	Symmetry	Linearity	N papers *
Pearson Correlation	Time	Covariance of time-series	Bivariate	Symmetric	Linear	18
Cross-Correlation	Time	Covariance of time-series	Bivariate	Asymmetric	Linear	8
Partial Correlation	Time	Covariance of time-series	Multivariate	Symmetric	Linear	12
Spearmans Rank Correlation	Time	Sum of squared differences	Bivariate	Symmetric	Linear/Non-Linear	4
Beta Series Correlation	Time	Covariance of regression coefficients	Bivariate	NA	NA	2
Dynamic Time Warping**	Time	Distance between points of input data	Bivariate	Symmetric	Linear	1
Amplitude Envelope Correlation	Time	Covariance of amplitude envelope of input signals	Bivariate	Symmetric	Linear	1
Fourier MSC	Frequency	Common strength of specific frequency	Bivariate	Symmetric	Linear	7
Wavelet MSC (WTC)	Time-Frequency	Common strength of specific frequency at specific time	Bivariate	Symmetric	Linear	91
Total Interdependence	Frequency	Mutual information between inputs	Bivariate	Symmetric	Linear	3
Imaginary Part of Coherence	Frequency	Phase relationship between inputs at specific frequency	Bivariate	Symmetric	Linear	1
Partial Wavelet Coherence	Time-Frequency	Common strength of specific frequency at specific time	Multivariate	Asymmetric	Linear	1
Mutual Coherence	Time-Frequency	Continuous regional pathways formed from phase differences	Multivariate	Asymmetric	Non-Linear	1
Phase Locking Value	Frequency	Phase Invariance	Bivariate	Symmetric	Linear	20
Interbrain Phase Coherence	Frequency	Phase Invariance	Bivariate	Symmetric	Linear	4
Integrative Coupling Index	Time-Frequency	Phase Invariance	Bivariate	Asymmetric	Linear	4
Phase Synchronization Index	Time-Frequency	Phase Invariance	Bivariate	Symmetric	Linear	3
Circular Correlation	Either	Covariance of phase variance	Bivariate	Symmetric	Linear	6
Weighted Phase Lag Index	Either	Asymmetry of distribution of phase differences	Bivariate	Asymmetric (if signed)	Linear	1
Granger Causality	Time	Variance of residuals	Bivariate	Asymmetric	Linear	1
Multivariate Granger Causality	Time	Variance of residuals	Multivariate	Asymmetric	Linear	1
Phase Slope Index	Frequency	Change in phase difference and coherence	Bivariate	Asymmetric	Non-Linear	1
Partial Directed Coherence	Either	Regression coefficients	Multivariate	Asymmetric	Linear	7
GLM Classification	Time	Distance between mean regression coefficients	Multivariate	Symmetric	Linear	1
Cross Brain GLM	Time	Regression coefficients	Multivariate	Asymmetric	Linear	6
PPI	Time	Regression Coefficients	Multivariate	Asymmetric	Linear	1
Bispectral Analysis	Frequency	Phase Invariance	Bivariate	Asymmetric	Non-Linear	1

* The total number of studies in the table is 187 since 5 studies used an unspecified 'correlation' and are not included.
** DTW can be non-linear and asymmetric depending on the step pattern used

metrics in the wider scientific context is challenging because they represent quite distinct things. This is even more compounded by using varying names for what is in essence the same method (see Section 5.4.3). Further to this, complexity in gauging IBC stems from the origin of methods being developed to account for problems surrounding single brain analysis. For example, many of the methods in Phase Synchrony are developed to deal with volume conduction occurring in one participant. The reason to use one of these methods over another is not clear, because volume conduction is not an issue when analysing the interaction between two channels from different sources. A more concerted effort by authors to specifically state the rationale of their chosen analytic method in assessing the underlying IBC would go far to aid in understanding why different methods are used, and what they represent in the context of the study at hand.

The majority of methods discovered in this review have their origin in single brain functional connectivity, where connectivity between regions is more intuitive to understand. This leads to a more fundamental issue in interpreting IBC results because these methods overlook the question of how the gap between the two-brains is bridged. A pure increase in IBC does not tell us much about the interaction itself, aside from the fact that there is an interaction (which is often inherent in the task). To gain a stronger cognitive interpretation of IBC data, it may be important to include accurate measures of participants behaviour during a hyperscanning task, because it is the coordination of behaviour which drives the hyperscanning effects (Hamilton, 2021). This means it is important to include multi-modal data in the experimental analysis (such as eye-tracking or motion capture). This requires the development of multivariate methods to facilitate analysis of these complex, interacting datasets; few studies have achieved this. A recent development from Guglielmini et al. (2022), (Guglielmini et al., 2022) incorporated multiple physiological recordings to evaluate how changes in behaviour (eye-contact), manifested in systemics (heart and breathing rates, electrodermal activity and blood pressure) and in the neural fNIRS data. They used WTC to determine coupling between: brain-brain, body-body and brain-body. This provides an intuitive link between changes in behaviour inducing changes in systemic physiology, inducing changes in the brain. Additionally the study from Cañigueral et al. (2021), incorporated eye-gaze and facial movements along with neural activity into a GLM to evaluate how partner behaviour is used to effect participants neural data.

With these thoughts in mind the ability of a neuroimaging modality to integrate multimodal information becomes an important consideration. The implementation of extra measuring equipment allows us to delineate if, and how, inter-brain coupling ties into reciprocal (and non-reciprocal) behaviour during an interaction, and the effect this has on a person's physiology, aiding in meaningful interpretations from the data. In this respect fNIRS and EEG are more suitable than the magnetic modalities since they do not require equipment which is MR safe, and similarly fNIRS is preferrable to EEG since it is robust against any electrical interference originating from the surroundings, (for example as discussed by Dikker et al. (2021)). This is an important perspective to consider when conducting more complex hyperscanning experiments.

Because wavelet coherence for fNIRS is by far the most commonly used method and modality for hyperscanning research, we consider the issues for this approach in a little more detail. When using any frequency/time-frequency based analysis, the choice of the frequency (or range of frequencies) to analyse is a crucial parameter to choose. With direct measures of neuronal activity, this choice has a direct implication, since different frequency bands (e.g. alpha, gamma) have specific theorized brain functions. However, with indirect measures such as fNIRS and fMRI the role frequencies play in the recorded signal is less clear. One possibility is that the frequencies in the signal are driven by the dynamics of the task that the participants are engaged in – participants in a rapid button pressing task might show different signal frequency compared to participants in a slow-moving trust-building conversation. In addition, it is known that each fNIRS signal is a combination of different physiological components, each with their own function (Tachtsidis and Scholkmann, 2016), however how these relate to the recorded brain function is unclear. The selection of frequency band used by studies using wavelet coherence is done in varying ways, including visual inspection (Li et al., 2020; Yuan et al., 2022), using the task-frequency (Osaka et al., 2015; Baker et al., 2016; Park, Shin and Jeong, 2022) or previous studies (Reindl et al., 2018). Other studies compute significance between real and permuted dyads for all frequencies and select frequencies showing significantly high coherence values (Zhao, Zhu and Hu, 2021; Zhu et al., 2022; Pan, Cheng and Hu, 2022; Sabino Guglielmini et al., 2022). However in other cases (Liu et al., 2019; Zhao et al., 2022) experimenters conduct paired t-tests between task and rest periods for all frequencies and base their analysis on frequencies with a significant difference between the task and rest. The use of methods such as visual inspection or significance testing between task and rest do not provide mechanistic justifications for the choice of frequency selection, rather differences are found first and analysis conducted after. This has substantial risk of double-dipping (Kriegeskorte et al., 2009) and should be avoided. Selection of frequency bands from an independent source or pre-registration of analysis of specific bands could be useful for future hyperscanning studies. Studies using frequency analyses as their method should provide a mechanistic justification for which frequency band they use in order to provide context for their analysis and to aid in future studies.

The issues regarding the application of hyperscanning to fNIRS speak to a wider issue of a lack of a consistent fNIRS hyperscanning pipeline. This issue has begun to be broached within EEG hyperscanning, with developments of a hyperscanning toolbox (Ayrolles et al., 2021) for all analytic methods, aswell as the proposition of a pipeline for developmental EEG hyperscanning using the PLV (Kayhan et al., 2022). Within fNIRS this has been addressed recently by Nguyen et al. (2021) with respect to parent-child hyperscanning using wavelet coherence. Additionally work from Zhang et al. (2020) suggests best mathematical practice when using the wavelet coherence to assess IBC. Importantly the pipelines from Nguyen et al. (2021), Kayhan et al. (2022) both provide pipelines for specific IBC methods; and a general pipeline including selecting the IBC metric which is best suited to specific questions is still lacking. The toolbox from Ayrolles et al. (2021) begins addressing that by providing an easy to use computational toolbox where users can explore different methods and their application to different thereotical forms of coupling.

7. Conclusion and future perspectives

In this review we have provided a comprehensive summary of the current methods used to compute metrics of IBC across different modalities and explained the underlying rationales, formulation and assumptions of each. We have identified wide variability in which analytic methods are used to evaluate IBC. This variability is dependent on the technical properties of the modality used, however variation also exists between studies using the same neuroimaging modality. In part this variation is due to the lack of clear agreement on what IBC reflects and as such there is no consensus on which method should be used to identify the mechanisms relating to it. Because of this variation, it is important that moving forward discussions take place with respect to the mechanistic basis for IBC, and how analytic methods can be used to reflect this in order to aid reproducibility and to place hyperscanning research in the wider scientific context.

As neuroimaging equipment becomes more portable, accessible and wearable there is an increased application towards naturalistic, out-of-the-lab hyperscanning experiments. This brings with it benefits in increased real-world validity, but also challenges in analysing data from less-controlled experiments. Experimentally, this requires methodologies to be expanded to incorporate data acquisition from multiple sources to adequately describe the scenario being investigated. From an analytic perspective, methods developed and applied to lab settings may

not be applicable to real-world situations. Therefore, this will require the development of advanced analytic techniques to evaluate IBC in the context of the experiment being conducted, and with the inclusion of multi-modal data.

Data and code availability statement

This review does not include/use any original data or code. For any data/code contained in any studies referenced, please refer to the original article for further information.

Funding

This work was supported by the EPSRC-funded UCL Centre for Doctoral Training in Intelligent, Integrated Imaging in Healthcase (i4Health, EP/S021930/1) (UH), JSPS KAKENHI 19H03985 (YO) and 20H04496 (YO), National Institute of Mental Health of the National Institutes of Health under award numbers R01MH107513 (PI JH); 1R01MH119430 (JH), the Wellcome Trust (212979/Z/18/Z) (PP,IT).

Declaration of Competing Interest

The authors declare no conflict of interest related to this work. IT is the founder and CEO of MetaboLight LTD.

Data availability

No data was used for the research described in the article.

Supplementary materials

Supplementary material associated with this article can be found, in the online version, at doi:10.1016/j.neuroimage.2023.120354.

References

Abe, M.O., et al., 2019. Neural correlates of online cooperation during joint force production. Neuroimage 191, 150–161. https://doi.org/10.1016/j.neuroimage.2019.02.003. Available at:

Acquadro, M.A.S., Congedo, M., De Riddeer, D., 2016. Music performance as an experimental approach to hyperscanning studies. Front. Hum. Neurosci. 10 https://doi.org/10.3389/fnhum.2016.00242. Available at:

Ahn, S., et al., 2018. Interbrain phase synchronization during turn-taking verbal interaction-a hyperscanning study using simultaneous EEG/MEG. Hum. Brain Mapp. 39 (1), 171–188. https://doi.org/10.1002/hbm.23834. Available at:

Akimoto, M., et al., 2021. Inter-brain synchronization during sandplay therapy: individual analyses. Front. Psychol. 12, 1–12. Available at: https://www.frontiersin.org/article/10.3389/fpsyg.2021.723211 (Accessed: 22 March 2022).

Anders, S., et al., 2011. Flow of affective information between communicating brains. Neuroimage 54 (1), 439–446. https://doi.org/10.1016/j.neuroimage.2010.07.004. Available at:

Astolfi, L., et al., 2010. Neuroelectrical hyperscanning measures simultaneous brain activity in humans. Brain Topogr. 23 (3), 243–256. https://doi.org/10.1007/s10548-010-0147-9. Available at:

Astolfi, L., et al., 2011. Imaging the social brain by simultaneous hyperscanning during subject interaction. IEEE Intell. Syst. 26 (5), 38–45. https://doi.org/10.1109/MIS.2011.61. Available at:

Ayrolles, A., et al., 2021. HyPyP: a hyperscanning python pipeline for inter-brain connectivity analysis. Soc. Cognit. Affect. Neurosci. 16 (1–2), 72–83. https://doi.org/10.1093/scan/nsaa141. Available at:

Azhari, A., et al., 2019. Parenting stress undermines mother-child brain-to-brain synchrony: a hyperscanning study. Sci. Rep. 9 (1), 11407. https://doi.org/10.1038/s41598-019-47810-4. Available at:

Azhari, A., Bizzego, A., Esposito, G., 2021. Father-child dyads exhibit unique inter-subject synchronization during co-viewing of animation video stimuli. Soc. Neurosci. 16 (5), 522–533. https://doi.org/10.1080/17470919.2021.1970016. Available at:

Babiloni, F., Astolfi, L., 2014. Social neuroscience and hyperscanning techniques: past, present and future. Neurosci. Biobehav. Rev. 0, 76–93. https://doi.org/10.1016/j.neubiorev.2012.07.006. Available at:

Baccalá, L.A., Sameshima, K., 2001. Partial directed coherence: a new concept in neural structure determination. Biol. Cybern. 84 (6), 463–474. https://doi.org/10.1007/PL00007990. Available at:

Baker, J.M., et al., 2016. Sex differences in neural and behavioral signatures of cooperation revealed by fNIRS hyperscanning. Sci. Rep. 6 (1), 26492. https://doi.org/10.1038/srep26492. Available at:

Balconi, M., et al., 2019. Cooperative leadership in hyperscanning. Brain and body synchrony during manager-employee interactions. Neuropsychol. Trends (26), 23–44. https://doi.org/10.7358/neur-2019-026-bal2. Available at:

Balconi, M., Bartolo, A., Fronda, G., 2020. Social hyperscanning with fNIRS: intra-brain and inter-brain connectivity for social, affective, and informative gestures reproduction. Gesture 19 (2–3), 196–222. https://doi.org/10.1075/gest.20013.bal. Available at:

Balconi, M., Crivelli, D., Cassioli, F., 2022. "'We will let you know": an assessment of digital vs. face-to-face job interviews via EEG connectivity analysis. Information 13 (7), 312. https://doi.org/10.3390/info13070312. Available at:

Balconi, M., Fronda, G., 2020a. Gesture in hyperscanning during observation. inter-brain connectivity. Neuropsychol. Trends (28), 59–81. https://doi.org/10.7358/neur-2020-028-bal2. Available at:

Balconi, M., Fronda, G., 2020b. The "gift effect" on functional brain connectivity. Inter-brain synchronization when prosocial behavior is in action. Sci. Rep. 10 https://doi.org/10.1038/s41598-020-62421-0. Available at:

Balconi, M., Fronda, G., 2020c. The use of hyperscanning to investigate the role of social, affective, and informative gestures in non-verbal communication. electrophysiological (EEG) and inter-brain connectivity evidence. Brain Sci. 10 (1) https://doi.org/10.3390/brainsci10010029. Available at:

Balconi, M., Fronda, G., Bartolo, A., 2021. Affective, social, and informative gestures reproduction in human interaction: hyperscanning and brain connectivity. J. Mot. Behav. 53 (3), 296–315. https://doi.org/10.1080/00222895.2020.1774490. Available at:

Balconi, M., Fronda, G., Vanutelli, M.E., 2019. Donate or receive? social hyperscanning application with fNIRS. Curr. Psychol. 38 (4), 991–1002. https://doi.org/10.1007/s12144-019-00247-4. Available at:

Balconi, M., Fronda, G., Vanutelli, M.E., 2020. When gratitude and cooperation between friends affect inter-brain connectivity for EEG. BMC Neurosci. 21 (1), 14. https://doi.org/10.1186/s12868-020-00563-7. Available at:

Balconi, M., Gatti, L., Vanutelli, M.E., 2018a. EEG functional connectivity and brain-to-brain coupling in failing cognitive strategies. Conscious. Cogn. 60, 86–97. https://doi.org/10.1016/j.concog.2018.03.001. Available at:

Balconi, M., Gatti, L., Vanutelli, M.E., 2018b. When cooperation goes wrong: brain and behavioural correlates of ineffective joint strategies in dyads. Int. J. Neurosci. 128 (2), 155–166. https://doi.org/10.1080/00207454.2017.1379519. Available at:

Balconi, M., Vanutelli, M.E., 2017. Brains in competition: improved cognitive performance and inter-brain coupling by hyperscanning paradigm with functional near-infrared spectroscopy. Front. Behav. Neurosci. 11 https://doi.org/10.3389/fnbeh.2017.00163. Available at:

Balconi, M., Vanutelli, M.E., 2017. Interbrains cooperation: hyperscanning and self-perception in joint actions. J. Clin. Exp. Neuropsychol. 39 (6), 607–620. https://doi.org/10.1080/13803395.2016.1253666. Available at:

Balconi, M., Vanutelli, M.E., 2018a. EEG hyperscanning and behavioral synchronization during a joint actions. Neuropsychol. Trends (24), 23–47. https://doi.org/10.7358/neur-2018-024-balc. Available at:

Balconi, M., Vanutelli, M.E., 2018b. Functional EEG connectivity during competition. BMC Neurosci. 19 (1), 63. https://doi.org/10.1186/s12868-018-0464-6. Available at:

Balconi, M., Vanutelli, M.E., Gatti, L., 2018. Functional brain connectivity when cooperation fails. Brain Cogn. 123, 65–73. https://doi.org/10.1016/j.bandc.2018.02.009. Available at:

Balters, S., et al., 2020. Capturing human interaction in the virtual age: a perspective on the future of fNIRS hyperscanning. Front. Hum. Neurosci. 14 https://doi.org/10.3389/fnhum.2020.588494. Available at:

Barnett, T.P., et al., 1971. Bispectrum analysis of electroencephalogram signals during waking and sleeping. Science. https://doi.org/10.1126/science.172.3981.401 [Preprint] Available at:

Barraza, P., Pérez, A., Rodríguez, E., 2020. Brain-to-brain coupling in the gamma-band as a marker of shared intentionality. Front. Hum. Neurosci. 14 https://doi.org/10.3389/fnhum.2020.00295. Available at:

Barreto, C., et al., 2021. A new statistical approach for fNIRS hyperscanning to predict brain activity of preschoolers' using teacher's. Front. Hum. Neurosci. 15. Available at: https://www.frontiersin.org/article/10.3389/fnhum.2021.622146 (Accessed: 22 March 2022).

Becchio, C., Sartori, L., Castiello, U., 2010. Toward you: the social side of actions. Curr. Dir. Psychol. Sci. 19 (3), 183–188. https://doi.org/10.1177/0963721410370131. Available at:

Bilek, E., et al., 2015. Information flow between interacting human brains: identification, validation, and relationship to social expertise. Proc. Natl. Acad. Sci. 112 (16), 5207–5212. https://doi.org/10.1073/pnas.1421831112. Available at:

Bruns, A., et al., 2000. Amplitude envelope correlation detects coupling among incoherent brain signals. Neuroreport 11 (7), 1509–1514.

Burgess, A.P., 2013. On the interpretation of synchronization in EEG hyperscanning studies: a cautionary note. Front. Hum. Neurosci. 7 https://doi.org/10.3389/fnhum.2013.00881. Available at:

Caballero-Gaudes, C., Reynolds, R.C., 2017. Methods for cleaning the BOLD fMRI signal. Neuroimage 154, 128–149. https://doi.org/10.1016/j.neuroimage.2016.12.018. Available at:

Cañigueral, R., et al., 2021. Facial and neural mechanisms during interactive disclosure of biographical information. Neuroimage 226, 117572. https://doi.org/10.1016/j.neuroimage.2020.117572. Available at:

Cassioli, F., Balconi, M., 2022. An electrophysiological study applied to remote learning: preliminary results from an hyperscanning paradigm. Neuropsychol. Trends (31), 55–72. https://doi.org/10.7358/neur-2022-031-cass. Available at:
Cha, K.-M., Lee, H.-C., 2019. A novel qEEG measure of teamwork for human error analysis: an EEG hyperscanning study. Nucl. Eng. Technol. 51 (3), 683–691. https://doi.org/10.1016/j.net.2018.11.009. Available at:
Chabin, T., et al., 2022. Interbrain emotional connection during music performances is driven by physical proximity and individual traits. Ann. N.Y. Acad. Sci. 1508 (1), 178–195. https://doi.org/10.1111/nyas.14711. Available at:
Chang, C., Glover, G.H., 2010. Time–frequency dynamics of resting-state brain connectivity measured with fMRI. Neuroimage 50 (1), 81–98. https://doi.org/10.1016/j.neuroimage.2009.12.011. Available at:
Chen, D., et al., 2022. Gamma-band neural coupling during conceptual alignment. Hum. Brain Mapp. https://doi.org/10.1002/hbm.25831 n/a(n/a) Available at:
Chen, M., et al., 2020. Neural alignment during face-to-face spontaneous deception: does gender make a difference? Hum. Brain Mapp. 41 (17), 4964–4981. https://doi.org/10.1002/hbm.25173. Available at:
Cheng, X., et al., 2019. Coordination elicits synchronous brain activity between co-actors: frequency ratio matters. Front. Neurosci. 13 https://doi.org/10.3389/fnins.2019.01071. Available at:
Cheng, X., et al., 2022. Integration of social status and trust through interpersonal brain synchronization. Neuroimage 246, 118777. https://doi.org/10.1016/j.neuroimage.2021.118777. Available at:
Cheng, X., Guo, B., Hu, Y., 2022. Distinct neural couplings to shared goal and action coordination in joint action: evidence based on fNIRS hyperscanning. Soc. Cognit. Affect. Neurosci. nsac022. https://doi.org/10.1093/scan/nsac022. Available at:
Cheng, X., Li, X., Hu, Y., 2015. Synchronous brain activity during cooperative exchange depends on gender of partner: a fNIRS-based hyperscanning study. Hum. Brain Mapp. 36 (6), 2039–2048. https://doi.org/10.1002/hbm.22754. Available at:
Ciaramidaro, A., et al., 2018. Multiple-brain connectivity during third party punishment: an EEG hyperscanning study. Sci. Rep. 8 (1), 6822. https://doi.org/10.1038/s41598-018-24416-w. Available at:
Coomans, E., et al., 2021. Intersubject EEG coherence in healthy dyads during individual and joint mindful breathing exercise: an EEG-based experimental hyperscanning study. Adv. Cogn. Psychol. 17, 250–260. https://doi.org/10.5709/acp-0334-7. Available at:
Crivelli, D., Balconi, M., 2017. Near-infrared spectroscopy applied to complex systems and human hyperscanning networking. Appl. Sci. 7 (9), 922. https://doi.org/10.3390/app7090922. Available at:
Cui, X., Bryant, D.M., Reiss, A.L., 2012. NIRS-based hyperscanning reveals increased interpersonal coherence in superior frontal cortex during cooperation. Neuroimage 59 (3), 2430–2437. https://doi.org/10.1016/j.neuroimage.2011.09.003. Available at:
Czeszumski, A., et al., 2020. Hyperscanning: a valid method to study neural inter-brain underpinnings of social interaction. Front. Hum. Neurosci. 14, 1–17. Available at: https://www.frontiersin.org/article/10.3389/fnhum.2020.00039 (Accessed: 5 May 2022).
Czeszumski, A., et al., 2022. Cooperative behavior evokes interbrain synchrony in the prefrontal and temporoparietal cortex: a systematic review and meta-analysis of fNIRS hyperscanning studies. eNeuro 9 (2). https://doi.org/10.1523/ENEURO.0268-21.2022 p. ENEURO.0268-21.2022 Available at:
Dai, B., et al., 2018. Neural mechanisms for selectively tuning in to the target speaker in a naturalistic noisy situation. Nat. Commun. 9 https://doi.org/10.1038/s41467-018-04819-z. Available at:
Dai, R., et al., 2018. Holistic cognitive and neural processes: a fNIRS-hyperscanning study on interpersonal sensorimotor synchronization. Soc. Cognit. Affect. Neurosci. 13 (11), 1141–1154. https://doi.org/10.1093/scan/nsy090. Available at:
Deng, X., et al., 2022. Adolescent social anxiety undermines adolescent-parent interbrain synchrony during emotional processing: a hyperscanning study. Int. J. Clin. Health Psychol. IJCHP 22 (3), 100329. https://doi.org/10.1016/j.ijchp.2022.100329. Available at:
Descorbeth, O., et al., 2020. Neural processes for live pro-social dialogue between dyads with socioeconomic disparity. Soc. Cognit. Affect. Neurosci. 15 (8), 875–887. https://doi.org/10.1093/scan/nsaa120. Available at:
Dikker, S., et al., 2017. Brain-to-brain synchrony tracks real-world dynamic group interactions in the classroom. Curr. Biol. 27 (9), 1375–1380. https://doi.org/10.1016/j.cub.2017.04.002. Available at:
Dikker, S., et al., 2021. Crowdsourcing neuroscience: Inter-brain coupling during face-to-face interactions outside the laboratory. Neuroimage 227, 117436. https://doi.org/10.1016/j.neuroimage.2020.117436. Available at:
Djalovski, A., et al., 2021. Human attachments shape interbrain synchrony toward efficient performance of social goals. Neuroimage 226, 117600. https://doi.org/10.1016/j.neuroimage.2020.117600. Available at:
Dodel, S., Tognoli, E., Kelso, J.A.S., 2020. Degeneracy and complexity in neuro-behavioral correlates of team coordination. Front. Hum. Neurosci. 14 https://doi.org/10.3389/fnhum.2020.00328. Available at:
Dommer, L., et al., 2012. Between-brain coherence during joint n-back task performance: a two-person functional near-infrared spectroscopy study. Behav. Brain Res. 234 (2), 212–222. https://doi.org/10.1016/j.bbr.2012.06.024. Available at:
Dravida, S., et al., 2020. Joint attention during live person-to-person contact activates rTPJ, including a sub-component associated with spontaneous eye-to-eye contact. Front. Hum. Neurosci. 14 https://doi.org/10.3389/fnhum.2020.00201. Available at:
Duan, H., et al., 2020. Is the creativity of lovers better? a behavioral and functional near-infrared spectroscopy hyperscanning study. Curr. Psychol. https://doi.org/10.1007/s12144-020-01093-5 [Preprint]. Available at:
Duan, L., et al., 2015. Cluster imaging of multi-brain networks (CIMBN): a general framework for hyperscanning and modeling a group of interacting brains. Front. Neurosci. 9 https://doi.org/10.3389/fnins.2015.00267. Available at:
Dumas, G., et al., 2010. Inter-brain synchronization during social interaction. PLoS One 5 (8), e12166. https://doi.org/10.1371/journal.pone.0012166. Available at:
Dumas, G., et al., 2011. From social behaviour to brain synchronization: review and perspectives in hyperscanning. IRBM 32 (1), 48–53. https://doi.org/10.1016/j.irbm.2011.01.002. Available at:
Dumas, G., et al., 2012. Anatomical connectivity influences both intra- and inter-brain synchronizations. PLoS One 7 (5), e36414. https://doi.org/10.1371/journal.pone.0036414. Available at:
Ellingsen, D.M., et al., 2022. Patient–clinician brain concordance underlies causal dynamics in nonverbal communication and negative affective expressivity. Transl. Psychiatry 12 (1), 1–9. https://doi.org/10.1038/s41398-022-01810-7. Available at:
Fallani, F.D.V., et al., 2010. Defecting or not defecting: how to "read" human behavior during cooperative games by EEG measurements. PLoS One 5 (12), e14187. https://doi.org/10.1371/journal.pone.0014187. Available at:
Fenwick, P., et al., 2019. Neural correlates of induced light experience during meditation: a pilot hyperscanning study. NeuroQuantology 17 (1), 31–41. https://doi.org/10.14704/nq.2019.17.1.1318. Available at:
Filho, E., et al., 2016. Hyperbrain features of team mental models within a juggling paradigm: a proof of concept. PeerJ 4, e2457. https://doi.org/10.7717/peerj.2457. Available at:
Fishburn, F.A., et al., 2018. Putting our heads together: interpersonal neural synchronization as a biological mechanism for shared intentionality. Soc. Cognit. Affect. Neurosci. 13 (8), 841–849. https://doi.org/10.1093/scan/nsy060. Available at:
Friston, K., 2009. Causal modelling and brain connectivity in functional magnetic resonance imaging. PLoS Biol. 7 (2), e1000033 https://doi.org/10.1371/journal.pbio.1000033. Available at:
Friston, K., Moran, R., Seth, A.K., 2013. Analysing connectivity with Granger causality and dynamic causal modelling. Curr. Opin. Neurobiol. 23 (2), 172–178. https://doi.org/10.1016/j.conb.2012.11.010. Available at:
Friston, K.J., et al., 1997. Psychophysiological and modulatory interactions in neuroimaging. Neuroimage 6 (3), 218–229. https://doi.org/10.1006/nimg.1997.0291. Available at:
Fronda, G., Balconi, M., 2020. The effect of interbrain synchronization in gesture observation: a fNIRS study. Brain Behav. 10 (7), e01663. https://doi.org/10.1002/brb3.1663. Available at:
Gamliel, H.N., et al., 2021. Inter-group conflict affects inter-brain synchrony during synchronized movements. Neuroimage 245, 118661. https://doi.org/10.1016/j.neuroimage.2021.118661. Available at:
Gel'fand, I.M., 1959. Calculation of the amount of information about a random function contained in another such function. Ann. Math. Soc. Transl. Ser. 2 (12), 199–246.
Geweke, J., 1982. Measurement of linear dependence and feedback between multiple time series. J. Am. Statist. Assoc. 77 (378), 304–313. https://doi.org/10.1080/01621459.1982.10477803. Available at:
Goelman, G., et al., 2019. Bidirectional signal exchanges and their mechanisms during joint attention interaction - a hyperscanning fMRI study. Neuroimage 242–254. https://doi.org/10.1016/j.neuroimage.2019.05.028, 198 Available at:
Goelman, G., Dan, R., 2017. Multiple-region directed functional connectivity based on phase delays. Hum. Brain Mapp. 38 (3), 1374–1386. https://doi.org/10.1002/hbm.23460. Available at:
Goldstein, P., et al., 2018. Brain-to-brain coupling during handholding is associated with pain reduction. Proc. Natl. Acad. Sci. 115 (11), E2528–E2537. https://doi.org/10.1073/pnas.1703643115. Available at:
Granger, C.W.J., 1969. Investigating causal relations by econometric models and cross-spectral methods. Econometrica 37 (3), 424–438. https://doi.org/10.2307/1912791. Available at:
Guevara, M.A., Corsi-Cabrera, M., 1996. EEG coherence or EEG correlation? Int. J. Psychophysiol. 23 (3), 145–153. https://doi.org/10.1016/S0167-8760(96)00038-4. Available at:
Guglielmini, S., et al., 2022. Cross-frequency coupling between brain and body biosignals: a systemic physiology augmented functional near-infrared spectroscopy hyperscanning study. Adv. Exp. Med. Biol. 1395, 171–176. https://doi.org/10.1007/978-3-031-14190-4_29. Available at:
Guglielmini, Sabino, et al., 2022. Systemic physiology augmented functional near-infrared spectroscopy hyperscanning: a first evaluation investigating entrainment of spontaneous activity of brain and body physiology between subjects. Neurophotonics 9 (2), 026601. https://doi.org/10.1117/1.NPh.9.2.026601. Available at:
Gugnowska, K., et al., 2022. Endogenous sources of interbrain synchrony in duetting pianists. Cereb. Cortex bhab469. https://doi.org/10.1093/cercor/bhab469. Available at:
Gumilar, I., et al., 2021. A comparative study on inter-brain synchrony in real and virtual environments using hyperscanning. Comput. Graph. 94, 62–75. https://doi.org/10.1016/j.cag.2020.10.003. Available at:
Gvirts, H.Z., Perlmutter, R., 2020. What guides us to neurally and behaviorally align with anyone specific? a neurobiological model based on fNIRS hyperscanning studies. Neurosci. Rev. J. Bringing Neurobiol. Neurol. Psychiatry 26 (2), 108–116. https://doi.org/10.1177/1073858419861912. Available at:
Hakim, U., et al., 2022. Investigation of functional near-infrared spectroscopy signal quality and development of the hemodynamic phase correlation signal. Neurophotonics 9 (2), 025001. https://doi.org/10.1117/1.NPh.9.2.025001. Available at:

Hamilton, A.F., de, C., Lind, F., 2016. Audience effects: what can they tell us about social neuroscience, theory of mind and autism? Cult. Brain 4 (2), 159–177. https://doi.org/10.1007/s40167-016-0044-5. Available at:
Hamilton, A.F.de C., 2021. Hyperscanning: Beyond the Hype. Neuron 109 (3), 404–407. https://doi.org/10.1016/j.neuron.2020.11.008.
Hasegawa, C., et al., 2016. Mu rhythm suppression reflects mother-child face-to-face interactions: a pilot study with simultaneous MEG recording. Sci. Rep. 6 (1), 34977. https://doi.org/10.1038/srep34977. Available at:
Hasson, U., et al., 2004. Intersubject synchronization of cortical activity during natural vision. Science 303 (5664), 1634–1640. https://doi.org/10.1126/science.1089506. Available at:
Hasson, U., Frith, C.D., 2016. Mirroring and beyond: coupled dynamics as a generalized framework for modelling social interactions. Philos. Trans. R. Soc. Lond. B Biol. Sci. 371 (1693), 20150366 https://doi.org/10.1098/rstb.2015.0366. Available at:
Hirsch, J., et al., 2017. Frontal temporal and parietal systems synchronize within and across brains during live eye-to-eye contact. Neuroimage 157, 314–330. https://doi.org/10.1016/j.neuroimage.2017.06.018. Available at:
Hirsch, J., et al., 2018. A cross-brain neural mechanism for human-to-human verbal communication. Soc. Cognit. Affect. Neurosci. 13 (9), 907–920. https://doi.org/10.1093/scan/nsy070. Available at:
Hirsch, J., et al., 2021. Interpersonal agreement and disagreement during face-to-face dialogue: an fNIRS investigation. Front. Hum. Neurosci. 14 https://doi.org/10.3389/fnhum.2020.606397. Available at:
Hirsch, J., et al., 2022. Neural correlates of eye contact and social function in autism spectrum disorder. PLoS One 17 (11), e0265798. https://doi.org/10.1371/journal.pone.0265798. Available at:
Hoehl, S., Fairhurst, M., Schirmer, A., 2021. Interactional synchrony: signals, mechanisms and benefits. Soc. Cognit. Affect. Neurosci. 16 (1–2), 5–18. https://doi.org/10.1093/scan/nsaa024. Available at:
Holmes, N., et al., 2023. Naturalistic hyperscanning with wearable magnetoencephalography. Sensors 23 (12), 5454. https://doi.org/10.3390/s23125454. Available at:
Holper, L., et al., 2013. The teaching and the learning brain: A cortical hemodynamic marker of teacher–student interactions in the socratic dialog. Int. J. Educ. Res. 59, 1–10. https://doi.org/10.1016/j.ijer.2013.02.002. Available at:
Holper, L., Scholkmann, F., Wolf, M., 2012. Between-brain connectivity during imitation measured by fNIRS. Neuroimage 63 (1), 212–222. https://doi.org/10.1016/j.neuroimage.2012.06.028. Available at:
Holroyd, C.B., 2022. Interbrain synchrony: on wavy ground. Trends Neurosci. 45 (5), 346–357. https://doi.org/10.1016/j.tins.2022.02.002. Available at:
Hoyniak, C.P., et al., 2021. Adversity is linked with decreased parent-child behavioral and neural synchrony. Dev. Cogn. Neurosci. 48 https://doi.org/10.1016/j.dcn.2021.100937. Available at:
Hu, Y., et al., 2018. Inter-brain synchrony and cooperation context in interactive decision making. Biol. Psychol. 133, 54–62. https://doi.org/10.1016/j.biopsycho.2017.12.005. Available at:
Ikeda, S., et al., 2017. Steady beat sound facilitates both coordinated group walking and inter-subject neural synchrony. Front. Hum. Neurosci. 11, 147. https://doi.org/10.3389/fnhum.2017.00147. Available at:
İşbilir, E., 2016. Investigating Brain-Brain Interactions of a Dyad using fNIR Hyperscanning during Joint Sentence Reading Task. International Symposium on Brain and Cognitive Science ISBCS, 2016. Turkey.
Jahng, J., et al., 2017. Neural dynamics of two players when using nonverbal cues to gauge intentions to cooperate during the Prisoner's Dilemma Game. Neuroimage 157, 263–274. https://doi.org/10.1016/j.neuroimage.2017.06.024. Available at:
Jammalamadaka, S.R., Sengupta, A., SenGupta, A., 1999. Topics In Circular Statistics-vol 5. World Scientific Publishing Company, Singapore, Singapore. Available at: http://ebookcentral.proquest.com/lib/ucl/detail.action?docID=1679584 (Accessed: 7 June 2023).
Jiang, J., et al., 2015. Leader emergence through interpersonal neural synchronization. Proc. Natl. Acad. Sci. 112 (14), 4274–4279. https://doi.org/10.1073/pnas.1422930112. Available at:
Kang, K., et al., 2022. Does music induce interbrain synchronization between a non-speaking youth with cerebral palsy (CP), a parent, and a neurologic music therapist? A brief report. Dev. Neurorehabilit. 0 (0), 1–7. https://doi.org/10.1080/17518423.2022.2051628. Available at:
Kawasaki, M., Kitajo, K., Yamaguchi, Y., 2018. Sensory-motor synchronization in the brain corresponds to behavioral synchronization between individuals. Neuropsychologia 119, 59–67. https://doi.org/10.1016/j.neuropsychologia.2018.07.026. Available at:
Kayhan, E., et al., 2022. DEEP: a dual EEG pipeline for developmental hyperscanning studies. Dev. Cogn. Neurosci. 54, 101104 https://doi.org/10.1016/j.dcn.2022.101104. Available at:
Kelsen, B.A., et al., 2022. What has social neuroscience learned from hyperscanning studies of spoken communication? a systematic review. Neurosci. Biobehav. Rev. 132, 1249–1262. https://doi.org/10.1016/j.neubiorev.2020.09.008. Available at:
Key, A.P., et al., 2022. Greater social competence is associated with higher interpersonal neural synchrony in adolescents with autism. Front. Hum. Neurosci. 15. Available at: https://www.frontiersin.org/article/10.3389/fnhum.2021.790085 (Accessed: 24 March 2022).
Khalil, A., Musacchia, G., Iversen, J.R., 2022. It takes two: interpersonal neural synchrony is increased after musical interaction. Brain Sci. 12 (3), 409. https://doi.org/10.3390/brainsci12030409. Available at:
King-Casas, B., et al., 2005. Getting to know you: reputation and trust in a two-person economic exchange. Science 308 (5718), 78–83. https://doi.org/10.1126/science.1108062. Available at:
Kinreich, S., et al., 2017. Brain-to-brain synchrony during naturalistic social interactions. Sci. Rep. 7 (1), 17060. https://doi.org/10.1038/s41598-017-17339-5. Available at:
Kirilina, E., et al., 2012. The physiological origin of task-evoked systemic artefacts in functional near infrared spectroscopy. Neuroimage 61 (1), 70–81. https://doi.org/10.1016/j.neuroimage.2012.02.074. Available at:
Kitzbichler, M.G., et al., 2009. Broadband criticality of human brain network synchronization. PLoS Comput. Biol. 5 (3), e1000314 https://doi.org/10.1371/journal.pcbi.1000314. Available at:
Koide, T., Shimada, S., 2018. Cheering enhances inter-brain synchronization between sensorimotor areas of player and observer: inter-brain synchronization in cheering. Jpn. Psychol. Res. 60 (4), 265–275. https://doi.org/10.1111/jpr.12202. Available at:
Koike, T., et al., 2016. Neural substrates of shared attention as social memory: a hyperscanning functional magnetic resonance imaging study. Neuroimage 125, 401–412. https://doi.org/10.1016/j.neuroimage.2015.09.076. Available at:
Koike, T., Tanabe, H.C., et al., 2019. Role of the right anterior insular cortex in joint attention-related identification with a partner. Soc. Cognit. Affect. Neurosci. 14 (10), 1131–1145. https://doi.org/10.1093/scan/nsz087. Available at:
Koike, T., Sumiya, M., et al., 2019. What makes eye contact special? neural substrates of on-line mutual eye-gaze: a hyperscanning fMRI study. eNeuro 6 (1). https://doi.org/10.1523/ENEURO.0284-18.2019. Available at:
Koike, T., Tanabe, H.C., Sadato, N., 2015. Hyperscanning neuroimaging technique to reveal the "two-in-one" system in social interactions. Neurosci. Res. 90, 25–32. https://doi.org/10.1016/j.neures.2014.11.006. Available at:
Konvalinka, I., Roepstorff, A., 2012. The two-brain approach: how can mutually interacting brains teach us something about social interaction? Front. Hum. Neurosci. 6, 215. https://doi.org/10.3389/fnhum.2012.00215. Available at:
Kriegeskorte, N., et al., 2009. Circular analysis in systems neuroscience: the dangers of double dipping. Nat. Neurosci. 12 (5), 535–540. https://doi.org/10.1038/nn.2303. Available at:
Krueger, F., et al., 2007. Neural correlates of trust. Proc. Natl. Acad. Sci. 104 (50), 20084–20089. https://doi.org/10.1073/pnas.0710103104. Available at:
Kruppa, J.A., et al., 2021. Brain and motor synchrony in children and adolescents with ASD—a fNIRS hyperscanning study. Soc. Cognit. Affect. Neurosci. 16 (1–2), 103–116. https://doi.org/10.1093/scan/nsaa092. Available at:
Kuhlen, A.K., Brennan, S.E., 2013. Language in dialogue: when confederates might be hazardous to your data. Psychon. Bull. Rev. 20 (1), 54–72. https://doi.org/10.3758/s13423-012-0341-8. Available at:
Lachaux, J.P., et al., 1999. Measuring phase synchrony in brain signals. Hum. Brain Mapp. 8 (4), 194–208. Available at: 10.1002/(sici)1097-0193(1999)8:4<194::aid-hbm4>3.0.co;2-c.
Léné, P., et al., 2021. Is there collaboration specific neurophysiological activation during collaborative task activity? an analysis of brain responses using electroencephalography and hyperscanning. Brain Behav. 11 (11), e2270. https://doi.org/10.1002/brb3.2270. Available at:
Leong, V., Schilbach, L., 2019. The promise of two-person neuroscience for developmental psychiatry: using interaction-based sociometrics to identify disorders of social interaction. Br. J. Psychiatry 215 (5), 636–638. https://doi.org/10.1192/bjp.2019.73. Available at:
Li, J., et al., 2021. Inter-brain synchronization is weakened by the introduction of external punishment. Soc. Cognit. Affect. Neurosci. nsab124. https://doi.org/10.1093/scan/nsab124. Available at:
Li, L., et al., 2020. Interpersonal neural synchronization during cooperative behavior of basketball players: a fNIRS-based hyperscanning study. Front. Hum. Neurosci. 14 https://doi.org/10.3389/fnhum.2020.00169. Available at:
Li, R., et al., 2021. Dynamic inter-brain synchrony in real-life inter-personal cooperation: a functional near-infrared spectroscopy hyperscanning study. Neuroimage 238, 118263. https://doi.org/10.1016/j.neuroimage.2021.118263. Available at:
Li, Y., et al., 2020. Dyad sex composition effect on inter-brain synchronization in face-to-face cooperation. Brain Imaging Behav. https://doi.org/10.1007/s11682-020-00361-z [Preprint]. Available at:
Li, Y., et al., 2021. Experiencing happiness together facilitates dyadic coordination through the enhanced interpersonal neural synchronization. Soc. Cognit. Affect. Neurosci. https://doi.org/10.1093/scan/nsab114 nsab114. Available at:
Liberati, A., et al., 2009. The PRISMA statement for reporting systematic reviews and meta-analyses of studies that evaluate healthcare interventions: explanation and elaboration. BMJ 339, b2700. https://doi.org/10.1136/bmj.b2700. Available at:
Lindenberger, U., et al., 2009. Brains swinging in concert: cortical phase synchronization while playing guitar. BMC Neurosci. 10 (1), 22. https://doi.org/10.1186/1471-2202-10-22. Available at:
Liu, D., et al., 2018. Interactive brain activity: review and progress on EEG-based hyperscanning in social interactions. Front. Psychol. 9. Available at: https://www.frontiersin.org/articles/10.3389/fpsyg.2018.01862. Accessed 11 May 2023.
Liu, J., et al., 2019. Interplay between prior knowledge and communication mode on teaching effectiveness: Interpersonal neural synchronization as a neural marker. Neuroimage 193, 93–102. https://doi.org/10.1016/j.neuroimage.2019.03.004. Available at:
Liu, N., et al., 2016. NIRS-based hyperscanning reveals inter-brain neural synchronization during cooperative jenga game with face-to-face communication. Front. Hum. Neurosci. 10 https://doi.org/10.3389/fnhum.2016.00082. Available at:
Liu, T., et al., 2017. Inter-brain network underlying turn-based cooperation and competition: a hyperscanning study using near-infrared spectroscopy. Sci. Rep. 7 (1), 8684. https://doi.org/10.1038/s41598-017-09226-w. Available at:
Liu, T., et al., 2021. Team-work, team-brain: exploring synchrony and team interdependence in a nine-person drumming task via multiparticipant hyperscanning

and inter-brain network topology with fNIRS. Neuroimage 237, 118147. https://doi.org/10.1016/j.neuroimage.2021.118147. Available at:
Liu, W., et al., 2019. Shared neural representations of syntax during online dyadic communication. Neuroimage 198, 63–72. https://doi.org/10.1016/j.neuroimage.2019.05.035. Available at:
Long, Y., et al., 2021. Interpersonal neural synchronization during interpersonal touch underlies affiliative pair bonding between romantic couples. Cereb. Cortex 31 (3), 1647–1659. https://doi.org/10.1093/cercor/bhaa316. Available at:
Lu, K., et al., 2019. Cooperation makes a group be more creative. Cereb. Cortex 29 (8), 3457–3470. https://doi.org/10.1093/cercor/bhy215. Available at:
Lu, K., et al., 2021. Educational diversity and group creativity: evidence from fNIRS hyperscanning. Neuroimage 243, 118564. https://doi.org/10.1016/j.neuroimage.2021.118564. Available at:
Lu, K., et al., 2022. The hyper-brain neural couplings distinguishing high-creative group dynamics: an fNIRS hyperscanning study. Cereb. Cortex bhac161. https://doi.org/10.1093/cercor/bhac161. Available at:
Lu, K., Hao, N., 2019. When do we fall in neural synchrony with others? Soc. Cognit. Affect. Neurosci. 14 (3), 253–261. https://doi.org/10.1093/scan/nsz012. Available at:
Lu, K., Qiao, X., Hao, N., 2019. Praising or keeping silent on partner's ideas: leading brainstorming in particular ways. Neuropsychologia 124, 19–30. https://doi.org/10.1016/j.neuropsychologia.2019.01.004. Available at:
Lu, K., Teng, J., Hao, N., 2020. Gender of partner affects the interaction pattern during group creative idea generation. Exp. Brain Res. 238 (5), 1157–1168. https://doi.org/10.1007/s00221-020-05799-7. Available at:
Lu, K., Yu, T., Hao, N., 2020. Creating while taking turns, the choice to unlocking group creative potential. Neuroimage 219, 117025. https://doi.org/10.1016/j.neuroimage.2020.117025. Available at:
Marriott Haresign, I., et al., 2021. Automatic classification of ICA components from infant EEG using MARA. Dev. Cogn. Neurosci. 52, 101024. https://doi.org/10.1016/j.dcn.2021.101024.
Mayseless, N., Hawthorne, G., Reiss, A.L., 2019. Real-life creative problem solving in teams: fNIRS based hyperscanning study. Neuroimage 203, 116161. https://doi.org/10.1016/j.neuroimage.2019.116161. Available at:
Mihanović, H., Orlić, M., Pasarić, Z., 2009. Diurnal thermocline oscillations driven by tidal flow around an island in the Middle Adriatic. J. Mar. Syst. 78, S157–S168. https://doi.org/10.1016/j.jmarsys.2009.01.021. Available at:
Miller, J.G., et al., 2019. Inter-brain synchrony in mother-child dyads during cooperation: an fNIRS hyperscanning study. Neuropsychologia 124, 117–124. https://doi.org/10.1016/j.neuropsychologia.2018.12.021. Available at:
Misaki, M., et al., 2021. Beyond synchrony: the capacity of fMRI hyperscanning for the study of human social interaction. Soc. Cognit. Affect. Neurosci. 16 (1–2), 84–92. https://doi.org/10.1093/scan/nsaa143. Available at:
Miyata, K., et al., 2021. Neural substrates for sharing intention in action during face-to-face imitation. Neuroimage 233, 117916. https://doi.org/10.1016/j.neuroimage.2021.117916. Available at:
Montague, P.R., et al., 2002. Hyperscanning: Simultaneous fMRI during linked social interactions. Neuroimage 16 (4), 1159–1164. https://doi.org/10.1006/nimg.2002.1150. Available at:
Mu, Y., Guo, C., Han, S., 2016. Oxytocin enhances inter-brain synchrony during social coordination in male adults. Soc. Cognit. Affect. Neurosci. 11 (12), 1882–1893. https://doi.org/10.1093/scan/nsw106. Available at:
Mu, Y., Han, S., Gelfand, M.J., 2017. The role of gamma interbrain synchrony in social coordination when humans face territorial threats. Soc. Cognit. Affect. Neurosci. 12 (10), 1614–1623. https://doi.org/10.1093/scan/nsx093. Available at:
Müller, V., Lindenberger, U., 2019. Dynamic orchestration of brains and instruments during free guitar improvisation. Front. Integr. Neurosci. 13 https://doi.org/10.3389/fnint.2019.00050. Available at:
Müller, V., Lindenberger, U., 2022. Probing associations between interbrain synchronization and interpersonal action coordination during guitar playing. Ann. N.Y. Acad. Sci. 1507 (1), 146–161. https://doi.org/10.1111/nyas.14689. Available at:
Müller, V., Ohström, K.R.P., Lindenberger, U., 2021. Interactive brains, social minds: neural and physiological mechanisms of interpersonal action coordination. Neurosci. Biobehav. Rev. 128, 661–677. https://doi.org/10.1016/j.neubiorev.2021.07.017. Available at:
Müller, V., Sänger, J., Lindenberger, U., 2013. Intra- and inter-brain synchronization during musical improvisation on the guitar. PLoS One 8 (9), e73852. https://doi.org/10.1371/journal.pone.0073852. Available at:
Müller, V., Sänger, J., Lindenberger, U., 2018. Hyperbrain network properties of guitarists playing in quartet. Ann. N.Y. Acad. Sci. 1423 (1), 198–210. https://doi.org/10.1111/nyas.13656. Available at:
Nam, C.S., et al., 2020. Brain-to-brain neural synchrony during social interactions: a systematic review on hyperscanning studies. Appl. Sci. 10 (19), 6669. https://doi.org/10.3390/app10196669. Available at:
Nguyen, T., et al., 2020. The effects of interaction quality on neural synchrony during mother-child problem solving. Cortex 124, 235–249. https://doi.org/10.1016/j.cortex.2019.11.020. Available at:
Nguyen, T., Schleihauf, H., Kungl, M., et al., 2021. Interpersonal neural synchrony during father–child problem solving: an fNIRS hyperscanning study. Child Dev. https://doi.org/10.1111/cdev.13510 n/a(n/a) Available at:
Nguyen, T., Schleihauf, H., Kayhan, E., et al., 2021. Neural synchrony in mother–child conversation: exploring the role of conversation patterns. Soc. Cognit. Affect. Neurosci. 16 (1–2), 93–102. https://doi.org/10.1093/scan/nsaa079. Available at:
Nguyen, T., Hoehl, S., Vrtička, P., 2021. A guide to parent-child fNIRS hyperscanning data processing and analysis. Sensors 21 (12), 4075. https://doi.org/10.3390/s21124075. Available at:
Niedermeyer, E., Silva, F.H.L.D., 2005. Electroencephalography: Basic Principles, Clinical Applications, and Related Fields. Lippincott Williams & Wilkins.
Noah, J.A., et al., 2020. Real-time eye-to-eye contact is associated with cross-brain neural coupling in angular gyrus. Front. Hum. Neurosci. 14 https://doi.org/10.3389/fnhum.2020.00019. Available at:
Nolte, G., et al., 2004. Identifying true brain interaction from EEG data using the imaginary part of coherency. Clin. Neurophysiol. 115 (10), 2292–2307. https://doi.org/10.1016/j.clinph.2004.04.029. Available at:
Nolte, G., et al., 2008. Robustly estimating the flow direction of information in complex physical systems. Phys. Rev. Lett. 100 (23), 234101 https://doi.org/10.1103/PhysRevLett.100.234101. Available at:
Nozawa, T., et al., 2016. Interpersonal frontopolar neural synchronization in group communication: an exploration toward fNIRS hyperscanning of natural interactions. Neuroimage 133, 484–497. https://doi.org/10.1016/j.neuroimage.2016.03.059. Available at:
Nozawa, T., et al., 2019. Prior physical synchrony enhances rapport and inter-brain synchronization during subsequent educational communication. Sci. Rep. 9 (1), 12747. https://doi.org/10.1038/s41598-019-49257-z. Available at:
Obrig, H., Villringer, A., 2003. Beyond the visible—imaging the human brain with light. J. Cereb. Blood Flow Metab. 23 (1), 1–18. https://doi.org/10.1097/01.WCB.0000043472.45775.29. Available at:
Oku, A.Y.A., et al., 2022. Applications of graph theory to the analysis of fNIRS data in hyperscanning paradigms. Front. Comput. Neurosci. 16. Available at: https://www.frontiersin.org/articles/10.3389/fncom.2022.975743 (Accessed: 4 October 2022).
Ono, Y., et al., 2021. Bidirectional connectivity between broca's area and wernicke's area during interactive verbal communication. Brain Connect. https://doi.org/10.1089/brain.2020.0790 [Preprint]. Available at:
O'Reilly, J.X., et al., 2012. Tools of the trade: psychophysiological interactions and functional connectivity. Soc. Cognit. Affect. Neurosci. 7 (5), 604–609. https://doi.org/10.1093/scan/nss055. Available at:
Osaka, N., et al., 2015. How two brains make one synchronized mind in the inferior frontal cortex: fNIRS-based hyperscanning during cooperative singing. Front. Psychol. 6, 1811. https://doi.org/10.3389/fpsyg.2015.01811. Available at:
Page, M.J., et al., 2021. The PRISMA 2020 statement: an updated guideline for reporting systematic reviews. BMJ 372, n71. https://doi.org/10.1136/bmj.n71. Available at:
Pan, Y., et al., 2017. Cooperation in lovers: an fNIRS-based hyperscanning study. Hum. Brain Mapp. 38 (2), 831–841. https://doi.org/10.1002/hbm.23421. Available at:
Pan, Y., et al., 2018. Interpersonal synchronization of inferior frontal cortices tracks social interactive learning of a song. Neuroimage 183, 280–290. https://doi.org/10.1016/j.neuroimage.2018.08.005. Available at:
Pan, Y., Dikker, S., et al., 2020. Instructor-learner brain coupling discriminates between instructional approaches and predicts learning. Neuroimage 211, 116657. https://doi.org/10.1016/j.neuroimage.2020.116657. Available at:
Pan, Y., Guyon, C., et al., 2020. Interpersonal brain synchronization with instructor compensates for learner's sleep deprivation in interactive learning. Biochem. Pharmacol., 114111 https://doi.org/10.1016/j.bcp.2020.114111. Available at:
Pan, Y., Cheng, X., Hu, Y., 2022. Three heads are better than one: cooperative learning brains wire together when a consensus is reached. Cereb. Cortex bhac127. https://doi.org/10.1093/cercor/bhac127. Available at:
Park, J., Shin, J., Jeong, J., 2022. Inter-brain synchrony levels according to task execution modes and difficulty levels: an fNIRS/GSR study. IEEE Trans. Neural Syst. Rehabil. Eng. 30, 194–204. https://doi.org/10.1109/TNSRE.2022.3144168. Available at:
Peng, W., et al., 2021. Suffer together, bond together: brain-to-brain synchronization and mutual affective empathy when sharing painful experiences. Neuroimage 238, 118249. https://doi.org/10.1016/j.neuroimage.2021.118249. Available at:
Pérez, A., et al., 2019. Differential brain-to-brain entrainment while speaking and listening in native and foreign languages. Cortex 111, 303–315. https://doi.org/10.1016/j.cortex.2018.11.026. Available at:
Pérez, A., Carreiras, M., Duñabeitia, J.A., 2017. Brain-to-brain entrainment: EEG interbrain synchronization while speaking and listening. Sci. Rep. 7 (1), 4190. https://doi.org/10.1038/s41598-017-04464-4. Available at:
Pinti, P., et al., 2019. Current status and issues regarding pre-processing of fNIRS neuroimaging data: an investigation of diverse signal filtering methods within a general linear model framework. Front. Hum. Neurosci. 12, 505. https://doi.org/10.3389/fnhum.2018.00505. Available at:
Pinti, P., et al., 2020. The present and future use of functional near-infrared spectroscopy (fNIRS) for cognitive neuroscience. Ann. N.Y. Acad. Sci. 1464 (1), 5–29. https://doi.org/10.1111/nyas.13948. Available at:
Pinti, P., et al., 2021. The role of anterior prefrontal cortex (area 10) in face-to-face deception measured with fNIRS. Soc. Cognit. Affect. Neurosci. 16 (1–2), 129–142. https://doi.org/10.1093/scan/nsaa086. Available at:
Piva, M., et al., 2017. Distributed neural activity patterns during human-to-human competition. Front. Hum. Neurosci. 11 https://doi.org/10.3389/fnhum.2017.00571. Available at:
Quaresima, V., Ferrari, M., 2019. Functional near-infrared spectroscopy (fNIRS) for assessing cerebral cortex function during human behavior in natural/social situations: a concise review. Organ. Res. Methods 22 (1), 46–68. https://doi.org/10.1177/1094428116658959. Available at:
Ratliff, E.L., et al., 2021. Into the unknown: examining neural representations of parent–adolescent interactions. Child Dev. 92 (6), e1361–e1376. https://doi.org/10.1111/cdev.13635. Available at:

Reindl, V., et al., 2018. Brain-to-brain synchrony in parent-child dyads and the relationship with emotion regulation revealed by fNIRS-based hyperscanning. Neuroimage 178, 493–502. https://doi.org/10.1016/j.neuroimage.2018.05.060. Available at:
Richard, C., et al., 2021. Elevated inter-brain coherence between subjects with concordant stances during discussion of social issues. Front. Hum. Neurosci. 15. Available at: https://www.frontiersin.org/article/10.3389/fnhum.2021.611886 (Accessed: 22 March 2022).
Rissman, J., Gazzaley, A., D'Esposito, M., 2004. Measuring functional connectivity during distinct stages of a cognitive task. Neuroimage 23 (2), 752–763. https://doi.org/10.1016/j.neuroimage.2004.06.035. Available at:
Saby, J.N., Marshall, P.J., 2012. The utility of EEG band power analysis in the study of infancy and early childhood. Dev. Neuropsychol. 37 (3), 253–273. https://doi.org/10.1080/87565641.2011.614663. Available at:
Saito, D.N., et al., 2010. Stay tuned": inter-individual neural synchronization during mutual gaze and joint attention. Front. Integr. Neurosci. 4 https://doi.org/10.3389/fnint.2010.00127. Available at:
Salazar, M., et al., 2021. You took the words right out of my mouth: dual-fMRI reveals intra- and inter-personal neural processes supporting verbal interaction. Neuroimage 228, 117697. https://doi.org/10.1016/j.neuroimage.2020.117697. Available at:
Sänger, J., Müller, V., Lindenberger, U., 2012. Intra- and interbrain synchronization and network properties when playing guitar in duets. Front. Hum. Neurosci. 6, 312. https://doi.org/10.3389/fnhum.2012.00312. Available at:
Sänger, J., Müller, V., Lindenberger, U., 2013. Directionality in hyperbrain networks discriminates between leaders and followers in guitar duets. Front. Hum. Neurosci. 7, 234. https://doi.org/10.3389/fnhum.2013.00234. Available at:
Santamaria, L., et al., 2020. Emotional valence modulates the topology of the parent-infant inter-brain network. Neuroimage 207, 116341. https://doi.org/10.1016/j.neuroimage.2019.116341. Available at:
Sato, J.R., et al., 2009. Frequency domain connectivity identification: an application of partial directed coherence in fMRI. Hum. Brain Mapp. 30 (2), 452–461. https://doi.org/10.1002/hbm.20513. Available at:
Schilbach, L., 2016. Towards a second-person neuropsychiatry. Philos. Trans. R. Soc. B Biol. Sci. 371 (1686), 20150081 https://doi.org/10.1098/rstb.2015.0081. Available at:
Scholkmann, F., et al., 2013. A new methodical approach in neuroscience: assessing inter-personal brain coupling using functional near-infrared imaging (fNIRI) hyperscanning. Front. Hum. Neurosci. 7 https://doi.org/10.3389/fnhum.2013.00813. Available at:
Scholkmann, F., et al., 2014. A review on continuous wave functional near-infrared spectroscopy and imaging instrumentation and methodology. Neuroimage 85, 6–27. https://doi.org/10.1016/j.neuroimage.2013.05.004. Available at:
Sciaraffa, N., et al., 2017. Brain interaction during cooperation: evaluating local properties of multiple-brain network. Brain Sci. 7 (7) https://doi.org/10.3390/brainsci7070090. Available at:
Sciaraffa, N., et al., 2021. Multivariate model for cooperation: bridging social physiological compliance and hyperscanning. Soc. Cognit. Affect. Neurosci. 16 (1–2), 193–209. https://doi.org/10.1093/scan/nsaa119. Available at:
Seth, A.K., Barrett, A.B., Barnett, L., 2015. Granger causality analysis in neuroscience and neuroimaging. J. Neurosci. 35 (8), 3293–3297. https://doi.org/10.1523/JNEUROSCI.4399-14.2015. Available at:
Seth, A.K., Chorley, P., Barnett, L.C., 2013. Granger causality analysis of fMRI BOLD signals is invariant to hemodynamic convolution but not downsampling. Neuroimage 65, 540–555. https://doi.org/10.1016/j.neuroimage.2012.09.049. Available at:
Shaw, D.J., et al., 2018. A dual-fMRI investigation of the iterated ultimatum game reveals that reciprocal behaviour is associated with neural alignment. Sci. Rep. 8 (1), 10896. https://doi.org/10.1038/s41598-018-29233-9. Available at:
Shehata, M., et al., 2021. Team flow is a unique brain state associated with enhanced information integration and interbrain synchrony. eNeuro 8 (5). https://doi.org/10.1523/ENEURO.0133-21.2021 p. ENEURO.0133-21.2021. Available at:
Shemyakina, N.V., Nagornova, Z.V., 2021. Neurophysiological characteristics of competition in skills and cooperation in creativity task Performance: a review of hyperscanning research. Hum. Physiol. 47 (1), 87–103. https://doi.org/10.1134/S0362119721010126.
Shiraishi, M., Shimada, S., 2021. Inter-brain synchronization during a cooperative task reflects the sense of joint agency. Neuropsychologia, 107770. https://doi.org/10.1016/j.neuropsychologia.2021.107770. Available at:
Zivan, M., et al., 2022. Reduced mother-child brain-to-brain synchrony during joint storytelling interaction interrupted by a media usage. Child Neuropsychol 0 (0), 1–20. https://doi.org/10.1080/09297049.2022.2034774.
Sievers B. et al. (2020) 'How consensus-building conversation changes our minds and aligns our brains'. PsyArXiv. Available at: doi:10.31234/osf.io/562z7.
Spiegelhalder, K., et al., 2014. Interindividual synchronization of brain activity during live verbal communication. Behav. Brain Res. 258, 75–79. https://doi.org/10.1016/j.bbr.2013.10.015. Available at:
Špiláková, B., et al., 2019. Dissecting social interaction: dual-fMRI reveals patterns of interpersonal brain-behavior relationships that dissociate among dimensions of social exchange. Soc. Cognit. Affect. Neurosci. 14 (2), 225–235. https://doi.org/10.1093/scan/nsz004. Available at:
Špiláková, B., et al., 2020. Getting into sync: data-driven analyses reveal patterns of neural coupling that distinguish among different social exchanges. Hum. Brain Mapp. 41 (4), 1072–1083. https://doi.org/10.1002/hbm.24861. Available at:
Stam, C.J., Nolte, G., Daffertshofer, A., 2007. Phase lag index: assessment of functional connectivity from multi channel EEG and MEG with diminished bias from common sources. Hum. Brain Mapp. 28 (11), 1178–1193. https://doi.org/10.1002/hbm.20346. Available at:
Stevens, R., Galloway, T.L., 2022. Exploring how healthcare teams balance the neurodynamics of autonomous and collaborative behaviors: a proof of concept. Front. Hum. Neurosci. 16 https://doi.org/10.3389/fnhum.2022.932468. Available at:
Stolk, A., et al., 2014. Cerebral coherence between communicators marks the emergence of meaning. Proc. Natl. Acad. Sci. U. S. A. 111 (51), 18183–18188. https://doi.org/10.1073/pnas.1414886111. Available at:
Sun, B., et al., 2020. Behavioral and brain synchronization differences between expert and novice teachers when collaborating with students. Brain Cogn. 139, 105513 https://doi.org/10.1016/j.bandc.2019.105513. Available at:
Sun, B., et al., 2021. Cooperation with partners of differing social experience: an fNIRS-based hyperscanning study. Brain Cogn. 154, 105803 https://doi.org/10.1016/j.bandc.2021.105803. Available at:
Szymanski, C., et al., 2017. Teams on the same wavelength perform better: inter-brain phase synchronization constitutes a neural substrate for social facilitation. Neuroimage 152, 425–436. https://doi.org/10.1016/j.neuroimage.2017.03.013. Available at:
Tachtsidis, I., Scholkmann, F., 2016. False positives and false negatives in functional near-infrared spectroscopy: issues, challenges, and the way forward. Neurophotonics 3 (3), 031405. https://doi.org/10.1117/1.NPh.3.3.031405. Available at:
Tang, H., et al., 2016. Interpersonal brain synchronization in the right temporo-parietal junction during face-to-face economic exchange. Soc. Cognit. Affect. Neurosci. 11 (1), 23–32. https://doi.org/10.1093/scan/nsv092. Available at:
Tang, Y., et al., 2020. Different strategies, distinguished cooperation efficiency, and brain synchronization for couples: An fNIRS-based hyperscanning study. Brain and Behavior 10 (9), e01768. https://doi.org/10.1002/brb3.1768. Available at:
Toppi, J., et al., 2016. Investigating cooperative behavior in ecological settings: an EEG hyperscanning study. PLoS One 11 (4), e0154236. https://doi.org/10.1371/journal.pone.0154236. Available at:
Torrence, C., Compo, G.P., 1998. A practical guide to wavelet analysis. Bull. Am. Meteorol. Soc. 79 (1), 61–78. https://doi.org/10.1175/1520-0477(1998)079<0061:APGTWA>2.0.CO;2. Available at:
Tsoi, L., et al., 2022. The promises and pitfalls of functional magnetic resonance imaging hyperscanning for social interaction research. Soc. Pers. Psychol. Compass 16 (10), e12707. https://doi.org/10.1111/spc3.12707. Available at:
Vinck, M., et al., 2011. An improved index of phase-synchronization for electrophysiological data in the presence of volume-conduction, noise and sample-size bias. Neuroimage 55 (4), 1548–1565. https://doi.org/10.1016/j.neuroimage.2011.01.055. Available at:
Wang, C., et al., 2019. Dynamic interpersonal neural synchronization underlying pain-induced cooperation in females. Hum. Brain Mapp. 40 (11), 3222–3232. https://doi.org/10.1002/hbm.24592. Available at:
Wang, L.S., et al., 2022. Distinct cerebral coherence in task-based fMRI hyperscanning: cooperation versus competition. Cereb. Cortex bhac075. https://doi.org/10.1093/cercor/bhac075. Available at:
Wang, M.Y., et al., 2018. Concurrent mapping of brain activation from multiple subjects during social interaction by hyperscanning: a mini-review. Quant. Imaging Med. Surg. 8 (8), 819–837. https://doi.org/10.21037/qims.2018.09.07. Available at:
Wang, Q., et al., 2020. Autism symptoms modulate interpersonal neural synchronization in children with autism spectrum disorder in cooperative interactions. Brain Topogr. 33 (1), 112–122. https://doi.org/10.1007/s10548-019-00731-x. Available at:
Wang, Z., et al., 2020. Interpersonal brain synchronization under bluffing in strategic games. Soc. Cognit. Affect. Neurosci. 15 (12), 1326–1335. https://doi.org/10.1093/scan/nsaa154. Available at:
Welch, P., 1967. The use of fast fourier transform for the estimation of power spectra: a method based on time averaging over short, modified periodograms. IEEE Trans. Audio Electroacoust. 15 (2), 70–73. https://doi.org/10.1109/TAU.1967.1161901. Available at:
Wen, X., Mo, J., Ding, M., 2012. Exploring resting-state functional connectivity with total interdependence. Neuroimage 60 (2), 1587–1595. https://doi.org/10.1016/j.neuroimage.2012.01.079. Available at:
Wu, S., et al., 2021. The only-child effect in the neural and behavioral signatures of trust revealed by fNIRS hyperscanning. Brain Cogn. 149, 105692 https://doi.org/10.1016/j.bandc.2021.105692. Available at:
Xie, H., et al., 2020. Finding the neural correlates of collaboration using a three-person fMRI hyperscanning paradigm. Proc. Natl. Acad. Sci. 117 (37), 23066–23072. https://doi.org/10.1073/pnas.1917407117. Available at:
Xue, H., Lu, K., Hao, N., 2018. Cooperation makes two less-creative individuals turn into a highly-creative pair. Neuroimage 172, 527–537. https://doi.org/10.1016/j.neuroimage.2018.02.007. Available at:
Yang, Q., et al., 2021. The underlying neural mechanisms of interpersonal situations on collaborative ability: a hyperscanning study using functional near-infrared spectroscopy. Soc. Neurosci. 16 (5), 549–563. https://doi.org/10.1080/17470919.2021.1965017. Available at:
Yoshioka, A., et al., 2021. Neural substrates of shared visual experiences: a hyperscanning fMRI study. Soc. Cognit. Affect. Neurosci. 16 (12), 1264–1275. https://doi.org/10.1093/scan/nsab082. Available at:
Yuan, D., et al., 2022. Interpersonal neural synchronization could predict the outcome of mate choice. Neuropsychologia 165, 108112. https://doi.org/10.1016/j.neuropsychologia.2021.108112. Available at:
Yun, K., Watanabe, K., Shimojo, S., 2012. Interpersonal body and neural synchronization as a marker of implicit social interaction. Sci. Rep. 2 (1), 959. https://doi.org/10.1038/srep00959. Available at:

Zhang, M., Liu, T., Pelowski, M., Yu, D, 2017. Gender difference in spontaneous deception: a hyperscanning study using functional near-infrared spectroscopy. Sci. Rep. 7 (1), 7508. https://doi.org/10.1038/s41598-017-06764-1. Available at:
Zhang, M., Jia, H., Zheng, M., 2020. Interbrain synchrony in the expectation of cooperation behavior: a hyperscanning study using functional near-infrared spectroscopy. Front. Psychol. 11, 542093 https://doi.org/10.3389/fpsyg.2020.542093. Available at:
Zhang, M., Liu, T., Pelowski, M., Jia, H., et al., 2017. Social risky decision-making reveals gender differences in the TPJ: a hyperscanning study using functional near-infrared spectroscopy. Brain Cogn. 119, 54–63. https://doi.org/10.1016/j.bandc.2017.08.008. Available at:
Zhang, M., et al., 2021. Group decision-making behavior in social dilemmas: inter-brain synchrony and the predictive role of personality traits. Person. Indiv. Differ. 168, 110315 https://doi.org/10.1016/j.paid.2020.110315. Available at:
Zhang, M., Jia, H., Wang, G., 2021. Interbrain synchrony of team collaborative decision-making: an fNIRS hyperscanning study. Front. Hum. Neurosci. 15. Available at: https://www.frontiersin.org/article/10.3389/fnhum.2021.702959 Accessed 22 March 2022.
Zhang, R., et al., 2021. Effects of acute psychosocial stress on interpersonal cooperation and competition in young women. Brain Cogn. 151, 105738 https://doi.org/10.1016/j.bandc.2021.105738. Available at:
Zamm, A., et al., 2021. Behavioral and neural dynamics of interpersonal synchrony between performing musicians: a wireless EEG hyperscanning study. Front. Hum. Neurosci. 15, 1–16. Available at: https://www.frontiersin.org/article/10.3389/fnhum.2021.717810 (Accessed: 22 March 2022).
Zhang, Y., et al., 2018. Interpersonal brain synchronization associated with working alliance during psychological counseling. Psychiatry Res. Neuroimaging 282, 103–109. https://doi.org/10.1016/j.pscychresns.2018.09.007. Available at:
Zhang, X., et al., 2020. Optimization of wavelet coherence analysis as a measure of neural synchrony during hyperscanning using functional near-infrared spectroscopy. Neurophotonics 7 (1), 015010. https://doi.org/10.1117/1.NPh.7.1.015010. Available at:
Zhang, Y., et al., 2020. Experience-dependent counselor-client brain synchronization during psychological counseling. eNeuro 7 (5). https://doi.org/10.1523/ENEURO.0236-20.2020. Available at:
Zhao, H., et al., 2021. How mother-child interactions are associated with a child's compliance. Cereb. Cortex 31 (9), 4398–4410. https://doi.org/10.1093/cercor/bhab094. Available at:
Zhao, H., et al., 2022. Inter-brain neural mechanism underlying turn-based interaction under acute stress in women: a hyperscanning study using functional near-infrared spectroscopy. Soc. Cognit. Affect. Neurosci. nsac005. https://doi.org/10.1093/scan/nsac005. Available at:
Zhao, N., Zhu, Y., Hu, Y., 2021. Inter-brain synchrony in open-ended collaborative learning: an fNIRS-hyperscanning study. J. Vis. Exp. JoVE (173). https://doi.org/10.3791/62777 [Preprint] Available at:
Zhao, Y., et al., 2017. Independent component analysis-based source-level hyperlink analysis for two-person neuroscience studies. J. Biomed. Opt. 22 (2), 027004 https://doi.org/10.1117/1.JBO.22.2.027004. Available at:
Zhdanov, A., et al., 2015. An internet-based real-time audiovisual link for dual MEG recordings. PLoS One 10 (6), e0128485. https://doi.org/10.1371/journal.pone.0128485. Available at:
Zhou, S., Long, Y., Lu, C., 2021. Measurement of the directional information flow in fNIRS-hyperscanning data using the partial wavelet transform coherence method. JoVE J. Vis. Exp. (175), e62927. https://doi.org/10.3791/62927. Available at:
Zhou, X., et al., 2021. Mortality threat mitigates interpersonal competition: an EEG-based hyperscanning study. Soc. Cognit. Affect. Neurosci. https://doi.org/10.1093/scan/nsab033 [Preprint]. Available at:
Zhu, Y., et al., 2022. Instructor–Learner Neural Synchronization During Elaborated Feedback Predicts Learning Transfer. J. Educ. Psychol. 114 (6), 1427–1441. https://doi.org/10.1037/edu0000707.

Further reading

Balconi, M., et al., 2020. Leader-employee emotional "interpersonal tuning". An EEG coherence study. Soc. Neurosci. 15 (2), 234–243 Available at: doi:10.1080/17470919.2019.1696226.